Automatica 132 (2021) 109809

Contents lists available at ScienceDirect

Automatica

journal homepage: www.elsevier.com/locate/automatica

Bounded-error target localization and tracking using a fleet of UAVs☆

Julius Ibenthal [a], Michel Kieffer [b], Luc Meyer [a,*], Hélène Piet-Lahanier [a], Sébastien Reynaud [a]

[a] Département Traitement de l'Information et Systèmes, ONERA, Univ Paris Saclay, 91120 Palaiseau, France
[b] Univ Paris-Saclay, CNRS, CentraleSupélec, Laboratoire des Signaux et Systèmes, 91192, Gif-sur-Yvette, France

ARTICLE INFO

Article history:
Received 13 March 2020
Received in revised form 21 December 2020
Accepted 4 June 2021
Available online 30 July 2021

Keywords:
Multi-agent systems
Collaborative systems
Multi-target tracking
Set membership estimation
Decision making and autonomy
Sensor data fusion
Autonomous systems

ABSTRACT

Among the various applications for fleets of UAVs, searching and tracking mobile targets remains a challenging task. In this paper, a distributed set-membership estimation and control scheme is presented. This scheme relies on the description of uncertainty and noise as bounded processes. Constraints on the field of view, as well as the presence of false targets, are taken into account. Each UAV maintains several set estimates: one for each detected and identified true target, one for detected but not yet identified targets, and one for not yet detected targets, which is also the subset of the state space still to be explored. These sets are updated by each UAV using the information coming from its sensors as well as received from its neighbors.

A distributed set-membership model predictive control approach is considered to compute the trajectories of UAVs. The control input minimizing a measure of the volume of the set-membership estimates predicted h-step ahead is then evaluated. Simulations of scenarios including the presence of false targets illustrate the ability of the proposed approach to efficiently search and track an unknown number of moving targets within some delimited search area.

1. Introduction

Among the various applications of fleets of UAVs, searching and tracking mobile targets in some geographic zone remains challenging. Numerous approaches have been developed in this context, see, *e.g.*, Khan, Rinner, and Cavallaro (2018) and Robin and Lacroix (2016) and the references therein. Most of the techniques of the state-of-the-art rely on a cooperative design of a search strategy and a distributed estimation of the target locations.

In this paper, we consider a fleet of UAVs, each of which being equipped with a sensor able to detect and localize targets from observations of a subset of the search area. When a target is detected, we assume that its identity is revealed only if some observation conditions are satisfied. This situation is typically encountered with cameras: the identity of a target is available only when it is observed from a satisfying point-of-view. We also account for the presence of moving false targets. These false targets may be erroneously identified as true targets and are distinguished from true targets only when observed under specific conditions. For each detected (true and false) target, we assume that some noisy measurement of its state is available. The noise corrupting the state observation is assumed to be bounded with known bounds, which may depend on the observation conditions.

We propose a robust distributed set-membership estimator run by each UAV. This estimator determines (*i*) set estimates containing the state of each *identified* target, (*ii*) a set estimate containing the states of *detected* but *not yet identified* (true and false) targets, and (*iii*) a set possibly containing targets remaining to be detected (the part of the search area still to be explored). The estimator is able to process measurements associated to detected but unidentified targets, prior to their identification at later time instants. The set estimator alternates predictions and corrections using measurements from the sensor of each UAV and measurements received during communications with its neighbors. The control inputs for each UAV are designed using a model predictive control (MPC) approach adapted to the set-membership estimation context, which aims at minimizing the volume of the set estimates. The MPC approach accounts for

☆ The authors gratefully thank the French *Agence de l'Innovation de Défense (AID)* for its fundings and the anonymous reviewers for their valuable suggestions. The material in this paper was partially presented at: the 57th IEEE Conference on Decision and Control, December 17–19, 2018, Miami Beach, Florida, USA. the 21st IFAC World Congress (IFAC 2020), July 12–17, 2020, Berlin, Germany. This paper was recommended for publication in revised form by Associate Editor Michael M. Zavlanos under the direction of Editor Christos G. Cassandras.

* Corresponding author.
E-mail addresses: julius.ibenthal@onera.fr, julius.ibenthal@gmx.de (J. Ibenthal), michel.kieffer@l2s.centralesupelec.fr (M. Kieffer), luc.meyer@onera.fr (L. Meyer), helene.piet-lahanier@onera.fr (H. Piet-Lahanier), sebastien.reynaud@onera.fr (S. Reynaud).

https://doi.org/10.1016/j.automatica.2021.109809
0005-1098/

the impact of future measurements on the set estimates and infers future information communicated by neighbors. A limited communication range is also considered.

In summary, the set-membership estimator proposed in this paper enables the detection and tracking of moving targets in presence of moving decoys. Issues related to false detection and misidentification of false targets, as well as potential non-identification of true targets are considered. The distinction between true and false targets relies on some deterministic observation conditions generalizing that introduced in Ibenthal, Meyer, Kieffer and Piet-Lahanier (2020) and Ibenthal, Meyer, Piet-Lahanier and Kieffer (2020). The distributed MPC approach introduced here accounts for limited and possibly delayed communications between UAVs, extending previous results in Ibenthal, Meyer, Kieffer et al. (2020) and Reboul, Kieffer, Piet-Lahanier, and Reynaud (2019). Finally, a better management of set estimates leads to a more efficient and computationally less demanding control law design compared to that of Ibenthal, Meyer, Kieffer et al. (2020).

Some related work in the context of cooperative search, acquisition, and track (CSAT) is provided in Section 2. Section 3 introduces notations and describes the way the CSAT problem is cast into a distributed set-membership estimation problem from bounded-error measurements. The evolution of set estimates for a given UAV and the way measurements are taken into account is described in Section 4. Section 5 introduces the considered distributed MPC approach, focusing on the various simplifications required to get a manageable complexity. Extended simulations are described in Section 6, before drawing some conclusions in Section 7.

2. Related work

In many papers, regarding CSAT problems, the estimation of target locations involves a probability map of the search zone. This map, shared between neighboring agents, represents the confidence of target locations (Bertuccelli & How, 2005; Yang, Polycarpou, & Minai, 2007). The prediction and update of the map are performed by recursive Bayesian filtering. UAV displacements are then designed to better update the map, as in Sun, Baek, and Pack (2014). In Khodayi-mehr, Kantaros, and Zavlanos (2019) and Zhang, Song, Huang, and Zhang (2017), communication constraints and limited fields of view (FoV) of the embedded sensors are taken into account. More recently, for effective tracking, a target assignment strategy has been proposed in Baek and York (2020). The assignment is updated with other cooperating agents using consensus decision-making.

Efficient search requires the design of control schemes to move the cooperative UAVs in order to optimize some criterion quantifying the performance of the search, *e.g.,* minimizing uncertainty of estimated target locations. A review of path-constrained approaches to design sets of trajectories is presented in Raap, Preuß, and Meyer-Nieberg (2019). These approaches rely on strong *a priori* knowledge on the search zone and on targets. Distributed optimal control strategies are proposed in Foraker, Royset, and Kaminer (2016a, 2016b), while game-theoretic techniques are considered in Li and Duan (2017). MPC is a well-adapted framework for designing controls optimizing a criterion while satisfying potential constraints which makes it a good candidate for defining search and track strategies as in Farmani, Sun, and Pack (2015) or Tokekar, Isler, and Franchi (2014). Better account of uncertainty in MPC is presented in Kouvaritakis and Cannon (2015).

Nevertheless, *a priori* probability density functions (pdfs) describing the process and measurement noises may not be always available. An alternative to the probabilistic description was proposed by Drevelle, Jaulin, and Zerr (2013) and Gu, He, and Han (2015). Instead of representing the target state estimate by a single point estimate, it was suggested to use a set-membership description of uncertainties. This description only assumes that a bounded support of the probability density function (pdf) of the measurement noise is available. Set estimates containing all possible states for a target are then derived, see Reboul et al. (2019) and Reynaud, Kieffer, Piet-Lahanier, and Reboul (2018). This type of bounded noise has been considered in the context of MPC, *e.g.*, in Bemporad and Garulli (2000), Canale, Fagiano, and Signorile (2014), and Ji and Driggs-Campbell (2020), and considered in a CSAT context in Ibenthal, Meyer, Kieffer et al. (2020), to the best of our knowledge.

Additional errors affecting CSAT may come from the fact that detected objects may not necessarily correspond to targets. Several approaches have been considered to model the uncertainty on the decision of considering a detected object as a target. In Bar-Shalom, Willett, and Tian (2011), Dames (2017) and Li and Duan (2017), a false alarm probability is introduced to account for the imperfect processing of the information acquired by sensors. Another possibility consists in considering the presence of decoys, *i.e.*, objects that can be considered as a true target when seen from a specific point of view. For example, Flint, Fernández, and Polycarpou (2004) introduce a Bayesian process for cooperative search when the sensors embedded on the UAVs are not able to determine whether a detected target is real or not. In He, Shin, and Tsourdos (2017), the random finite set probability density is used to model both target-generated observation and false alarms. An interactive multi-model filter is then used to estimate the modes of the detected objects. Detection or identification can be linked to some additional observation conditions not only depending on the field of view but also on the relative orientation of robot and target. A cooperative multirobot observation of multiple moving targets problem is considered in Pan et al. (2017) where the detection of a target depends on the target heading angle. There are less works addressing the CSAT problems considering that the target identity is revealed when some additional observation conditions are satisfied. Some results have been obtained in Blasch and Kahler (2005), where simultaneous target tracking and identification from electro-optical and infrared sensors is considered. In Ibenthal, Meyer, Kieffer et al. (2020) the presence of static decoys is taken into account, and the bounded-error approach introduced in Reynaud et al. (2018) is adapted to design a distributed set-membership estimator able to discriminate decoys from true targets.

3. Problem formulation

This paper addresses the problem of searching and tracking targets which can be identified based on some of their features, *e.g.*, license plates for cars, face characteristics for humans. One assumes that a unique identifier may be associated to each target and that the set $\mathcal{J}^{\mathrm{t}}$ of target identifiers is known *a priori*.

A fleet of N_{u} UAVs searches and tracks an unknown number $N_{\mathrm{t}} \leqslant \left|\mathcal{J}^{\mathrm{t}}\right|$ of targets moving within a limited area of interest. Furthermore, this area of interest also contains possibly moving decoys, called *false* targets hereafter. The set $\mathcal{J}^{\mathrm{f}}$ of false target identifiers is unknown but assumed to be such that $\mathcal{J}^{\mathrm{t}} \cap \mathcal{J}^{\mathrm{f}} = \emptyset$.

Table 1 provides the main notations used in this paper.

3.1. UAV and target states

At time $t = kT$, where T is the discretization time period, let $\mathbf{x}^{\mathrm{u}}_{i,k} \in \mathbb{R}^{n_{\mathrm{u}}}$ be the state vector of UAV i, $\mathbf{x}^{\mathrm{t}}_{j,k} \in \mathbb{R}^{n_{\mathrm{t}}}$ the state vector of target $j \in \mathcal{J}^{\mathrm{t}}$, and $\mathbf{x}^{\mathrm{f}}_{\ell,k} \in \mathbb{R}^{n_{\mathrm{t}}}$ the state vector of false target $\ell \in \mathcal{J}^{\mathrm{f}}$.

Table 1
Used variable and their definitions.

Variable	Definition
N_u, N_t, N_f	Number of UAVs, true, and false targets
n_u , n_t	State vector size for UAVs and true targets
$\mathbf{x}^u_{i,k}$	State vector of UAV i at time k
$\mathbf{x}^t_{j,k}$, $\mathbf{x}^f_{\ell,k}$	State vector of true j and false target ℓ at time k
$\mathbf{f}^u_k$, $\mathbf{f}^t_k$	Dynamical model of UAVs and targets
$\mathbf{v}_{j,k} \in [\mathbf{v}_k]$	True target state perturbations
$\mathbf{u}_{i,k} \in \mathbb{U}$	UAV i control input at time k
$\mathbb{X}_0$	Initial set of true and false target states
$\mathbb{F}_i(\mathbf{x}^u_{i,k}) \subset \mathbb{R}^{n_t}$	Observed subset by UAV i
$\mathbf{h}_i\left(\mathbf{x}^u_{i,k}, \mathbf{x}^t_{j,k}\right)$	Observation equation of UAV i at time k
$\mathbf{y}^I_{i,j,k}$	Measurement of the identified true target $j \in \mathcal{D}^I_{i,k}$
$\mathbf{y}^U_{i,m,k}$	Measurement of the unidentified true target $m \in \mathcal{D}^U_{i,k}$ such that $j = \pi^{-1}_{i,k}(m) \in \mathcal{J}^t$
$\mathbf{w}_{i,j,k} \in [\mathbf{w}_{i,k}]$	Observation noise
$\mathbf{x}^t_{j,k} \in \mathbb{F}_i\left(\mathbf{x}^u_{i,k}\right)$	Detection condition for true targets
$\mathbf{x}^f_{\ell,k} \in \mathbb{F}_i\left(\mathbf{x}^u_{i,k}\right)$	Detection condition for false targets
$g^t_j\left(\mathbf{x}^u_{i,k}, \mathbf{x}^t_{j,k}\right) \geqslant 0$	Identifiability condition for true targets
$g^f_\ell\left(\mathbf{x}^u_{i,k}, \mathbf{x}^f_{\ell,k}\right) \geqslant 0$	Identifiability condition for false targets
$q^f_\ell\left(\mathbf{x}^u_{i,k}, \mathbf{x}^f_{\ell,k}\right) \geqslant 0$	Confusion condition for false targets
$\pi_{i,k}(j)$, $\pi_{i,k}(\ell)$	Unknown mapping from $\mathcal{J}^t \cup \mathcal{J}^f$ to $\mathbb{N}$
$\mathcal{L}_{i,k}$	List of known identified targets by UAV i at time k
$\mathcal{D}^I_{i,k}$	Set of detected and identified targets and misidentified false targets by UAV i at time k
$\mathcal{D}^U_{i,k}$	Set of integers referring to true and false targets that were detected but not identified
$\mathcal{N}_{i,k}$	Set of neighbors connected to UAVi at time k
$\mathbb{X}_{i,j,k}$	Set estimate for target j by UAV i at time k
$\mathbb{X}^U_{i,k}$	Set estimate for unidentified targets by UAV i at time k
$\mathcal{X}_{i,k}$	List of set estimates by UAV i at time k
$\overline{\mathbb{X}}_{i,k}$	Set still to be explored
$\phi(\mathbb{A})$	Measure of set $\mathbb{A}$
$\overline{\Phi}_k$	Average estimation uncertainty at time k

The evolution with time of the state of UAVs and true targets is modeled as

$$\mathbf{x}^u_{i,k+1} = \mathbf{f}^u_k\left(\mathbf{x}^u_{i,k}, \mathbf{u}_{i,k}\right), \tag{1}$$

$$\mathbf{x}^t_{j,k+1} = \mathbf{f}^t_k\left(\mathbf{x}^t_{j,k}, \mathbf{v}_{j,k}\right), \tag{2}$$

where $\mathbf{u}_{i,k}$ is the control input for UAV i, to be chosen in a set $\mathbb{U}$ of admissible control inputs; $\mathbf{v}_{j,k}$ is an unknown target state perturbation belonging to the known box $[\mathbf{v}_k]$. No particular assumption is considered about the evolution of $\mathbf{x}^f_{\ell,k}$: false targets may be static or moving. The UAVs search and track targets only within the area of interest $\mathbb{X}_0 \subset \mathbb{R}^{n_t}$.

3.2. Measurements

All UAVs are equipped with sensors able to observe a subset of the area of interest $\mathbb{X}_0$. A true or false target is always *detected* by UAV i if the target state belongs to the observed subset (Field of View, FoV) $\mathbb{F}_i(\mathbf{x}^u_{i,k}) \subset \mathbb{X}_0 \subset \mathbb{R}^{n_t}$, *i.e.*, if $\mathbf{x}^t_{j,k} \in \mathbb{F}_i(\mathbf{x}^u_{i,k})$ or $\mathbf{x}^f_{\ell,k} \in \mathbb{F}_i(\mathbf{x}^u_{i,k})$.

When a true target is detected, two cases may occur depending on an additional *identification* condition g^t. If condition g^t is satisfied, then the target is recognized as a true target and its unique identifier $j \in \mathcal{J}^t$ is obtained. If the condition g^t is not satisfied, then no information on the target's identity is available: the UAV does not know if the detected object is a true or a false target. We assume that misidentification does not occur for true targets.

When a false target $\ell \in \mathcal{J}^f$ is detected and an identification condition g^f holds, an identifier j is obtained, which may not necessarily be equal to ℓ. A misidentification may occur depending on an additional condition q^f. If q^f is satisfied, the obtained identifier is $J(\ell) \in \mathcal{J}^t$, where J is some deterministic *confusion* function, *i.e.*, a false target is always confused with the same true target. If q^f is not satisfied, then the obtained identifier is $\ell \in \mathcal{J}^f$, which allows the UAV to determine that a false target is detected. When g^f is not satisfied, the UAV does not know if the detected target is a true or a false target and does not have access to its identifier.

More formally, at time k, UAV i obtains two lists $\mathcal{D}^I_{i,k}$, and $\mathcal{D}^U_{i,k}$ from the information gathered in $\mathbb{F}_i(\mathbf{x}^u_{i,k})$.

$\mathcal{D}^I_{i,k} \subset \mathcal{J}^t$ contains the identifiers of all true targets that are detected and identified at time k, *i.e.*,

$$\mathbf{x}^t_{j,k} \in \mathbb{F}_i\left(\mathbf{x}^u_{i,k}\right) \wedge g^t_j\left(\mathbf{x}^u_{i,k}, \mathbf{x}^t_{j,k}\right) \geqslant 0 \Rightarrow j \in \mathcal{D}^I_{i,k}, \tag{3}$$

where g^t_j is the identification condition for the true target j. $\mathcal{D}^I_{i,k}$ also contains the identifiers of all false targets that were detected and misidentified, and so confused with a target $j \in \mathcal{J}^t$ at time k, *i.e.*,

$$\mathbf{x}^f_{\ell,k} \in \mathbb{F}_i\left(\mathbf{x}^u_{i,k}\right) \wedge g^f_\ell\left(\mathbf{x}^u_{i,k}, \mathbf{x}^f_{\ell,k}\right) \geqslant 0 \wedge q^f_\ell\left(\mathbf{x}^u_{i,k}, \mathbf{x}^f_{\ell,k}\right) \geqslant 0 \Rightarrow J(\ell) \in \mathcal{D}^I_{i,k}, \tag{4}$$

where g^f_ℓ and q^f_ℓ are the identification and misidentification conditions for the false target ℓ. An identifier j may appear multiple times in $\mathcal{D}^I_{i,k}$ due to the potential presence of a true target and one or more false targets confused with that true target in the FoV of the UAV.

$\mathcal{D}^U_{i,k}$ is a list of integers referring to true and false targets that are detected but not identified (conditions g^t and g^f are not satisfied). For a true target $j \in \mathcal{J}^t$

$$\mathbf{x}^t_{j,k} \in \mathbb{F}_i\left(\mathbf{x}^u_{i,k}\right) \wedge g^t_j\left(\mathbf{x}^u_{i,k}, \mathbf{x}^t_{j,k}\right) < 0 \Rightarrow \pi_{i,k}(j) \in \mathcal{D}^U_{i,k},$$

where $\pi_{i,k}$ maps $\mathcal{J}^t \cup \mathcal{J}^f$ to $\mathbb{N}$. For a false target $\ell \in \mathcal{J}^f$

$$\mathbf{x}^f_{\ell,k} \in \mathbb{F}_i\left(\mathbf{x}^u_{i,k}\right) \wedge g^f_\ell\left(\mathbf{x}^u_{i,k}, \mathbf{x}^f_{\ell,k}\right) < 0 \Rightarrow \pi_{i,k}(\ell) \in \mathcal{D}^U_{i,k}.$$

The function $\pi_{i,k}$ is used to assign an integer to the index of unidentified targets in the order they are processed $\mathcal{D}^U_{i,k} = \{1, 2, 3, \ldots\}$. For example $\mathcal{D}^U_{i,k} = \{1, 2, 3\}$ indicates that three unidentified targets are detected at time k by UAV i.

The UAVs are not aware of the structure of g^t_j, g^f_ℓ, and q^f_ℓ. The condition $g^t_j(\mathbf{x}^u_{i,k}, \mathbf{x}^t_{j,k}) \geqslant 0$ may represent a situation where the UAV i identifies the true target since it is observed from some specific point of view belonging, for example, to some polyhedral cone whose apex is $\mathbf{x}^t_{j,k}$. A similar structure is assumed for the identification condition g^f_ℓ for false targets. The misidentification condition $q^f_\ell(\mathbf{x}^u_{i,k}, \mathbf{x}^f_{\ell,k}) \geqslant 0$ is satisfied if, for example, UAV i does not belong to some polyhedral cone whose apex is $\mathbf{x}^f_{\ell,k}$. Similar identification conditions have been proposed in Pan et al. (2017). Figs. 1 and 2 show the measurement process and the information obtained depending on the fulfilled conditions. Fig. 3 illustrates different scenarios when a target is detected. The red UAV detects and identifies the false target ℓ_1 as $\mathbf{x}^f_{\ell_1,k} \in \mathbb{F}_i(\mathbf{x}^u_{i,k})$ and $g^f_{\ell_1}(\mathbf{x}^u_{i,k}, \mathbf{x}^f_{\ell_1,k}) \geqslant 0$. Moreover, target ℓ_1 is correctly identified as a false target as $q^f_{\ell_1}(\mathbf{x}^u_{i,k}, \mathbf{x}^f_{\ell_1,k}) < 0$. The green UAV detects and identifies the true target j_1 correctly as $\mathbf{x}^t_{j_1,k} \in \mathbb{F}_i(\mathbf{x}^u_{i,k})$ and $g^t_{j_1}(\mathbf{x}^u_{i,k}, \mathbf{x}^t_{j_1,k}) \geqslant 0$. The blue UAV detects the true target j_2 as $\mathbf{x}^t_{j_2,k} \in \mathbb{F}_i(\mathbf{x}^u_{i,k})$ but it is not identified since $g^t_{j_2}(\mathbf{x}^u_{i,k}, \mathbf{x}^t_{j_2,k}) < 0$. Finally, the blue UAV detects and identifies the false target ℓ_2 as $\mathbf{x}^f_{\ell_2,k} \in \mathbb{F}_i(\mathbf{x}^u_{i,k})$ and $g^f_{\ell_2}(\mathbf{x}^u_{i,k}, \mathbf{x}^f_{\ell_2,k}) \geqslant 0$, but it is confused with a true target since $q^f_{\ell_2}(\mathbf{x}^u_{i,k}, \mathbf{x}^f_{\ell_2,k}) \geqslant 0$.

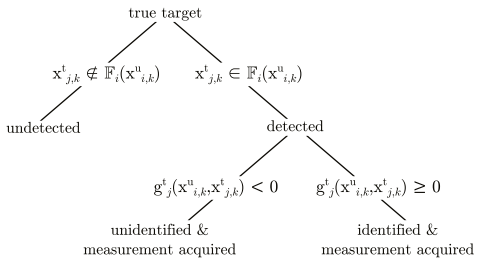

Fig. 1. Measurement process for true targets: the figure shows the obtained information on true targets depending on the observation conditions and identification condition g^t_j.

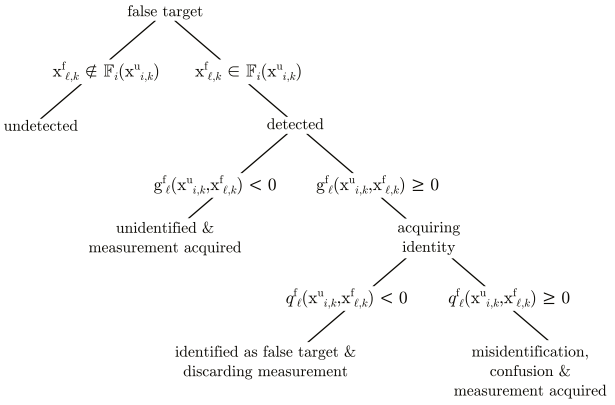

Fig. 2. Measurement process for false targets: the figure shows the obtained information on false targets depending on the observation conditions, the identification condition g^f_ℓ, and the misidentification condition q^f_ℓ.

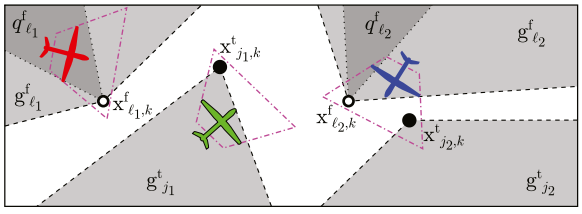

Fig. 3. Projection of the 2D plane (x_1, x_2) of the area of interest, of the state of true targets $\mathbf{x}^t_{i,k}$ (filled circles) and false targets $\mathbf{x}^f_{\ell,k}$ (empty circles). The subsets defined by $g^t_j(\mathbf{x}^u_{i,k}, \mathbf{x}^t_{j,k}) \geqslant 0$ and $g^f_\ell(\mathbf{x}^u_{i,k}, \mathbf{x}^f_{\ell,k}) \geqslant 0$ where targets can be identified are illustrated by the projection of the conic subspace in light gray. The subset defined by $q^f_\ell(\mathbf{x}^u_{i,k}, \mathbf{x}^f_{\ell,k}) < 0$ where false targets are identified as false targets is represented by the projection of the conic subspace in dark gray. The boundary of the FoV is in dashed-dotted magenta.

A noisy observation of the state $\mathbf{x}^t_{j,k}$ is obtained for each identified true target $j \in \mathcal{D}^I_{i,k}$ as

$$\mathbf{y}^I_{i,j,k} = \mathbf{h}_i\left(\mathbf{x}^u_{i,k}, \mathbf{x}^t_{j,k}\right) + \mathbf{w}_{i,j,k}, \tag{5}$$

and for each unidentified true target $m \in \mathcal{D}^U_{i,k}$ such that $j = \pi^{-1}_{i,k}(m) \in \mathcal{J}^t$, as

$$\mathbf{y}^U_{i,m,k} = \mathbf{h}_i\left(\mathbf{x}^u_{i,k}, \mathbf{x}^t_{j,k}\right) + \mathbf{w}_{i,j,k}, \tag{6}$$

where $\mathbf{h}_i$ is the observation equation of UAV i and $\mathbf{w}_{i,j,k}$ represents some measurement noise, bounded in some box $[\mathbf{w}_{i,j,k}]$. Usually the size of this box varies according to environmental and measurement conditions and is unknown (Cortes, Martinez, Karatas, & Bullo, 2004; Li & Duan, 2017). One assumes, however, that a known box $[\mathbf{w}_{i,k}]$ such that $[\mathbf{w}_{i,j,k}] \subset [\mathbf{w}_{i,k}]$ can be obtained, considering, *e.g.*, worst-case measurement conditions.

A noisy observation of the state $\mathbf{x}^f_{\ell,k}$ of false targets ℓ, which are misidentified, *i.e.*, $J(\ell) \in \mathcal{D}^I_{i,k}$, is obtained as

$$\mathbf{y}^I_{i,J(\ell),k} = \mathbf{h}_i\left(\mathbf{x}^u_{i,k}, \mathbf{x}^f_{\ell,k}\right) + \mathbf{w}_{i,\ell,k}, \tag{7}$$

and of unidentified false targets $m \in \mathcal{D}^U_{i,k}$ such that $\ell = \pi^{-1}_{i,k}(m) \in \mathcal{J}^f$, as

$$\mathbf{y}^U_{i,m,k} = \mathbf{h}_i\left(\mathbf{x}^u_{i,k}, \mathbf{x}^f_{\ell,k}\right) + \mathbf{w}_{i,\ell,k}, \tag{8}$$

where $\mathbf{w}_{i,\ell,k}$ belongs to some box $[\mathbf{w}_{i,\ell,k}]$. One assumes again that a known box $[\mathbf{w}_{i,k}]$ is available such that $[\mathbf{w}_{i,\ell,k}] \subset [\mathbf{w}_{i,k}]$.

As illustrated in Section 4.2 measurements and noise bounds are used to get set estimates of the target locations. After a first estimate is obtained from conservative noise bounds, if there is a *known* dependency between the noise bounds and the distance to the target, it may be possible to get more accurate noise bounds. These refined bounds may then be used to reduce the size of the set estimate of the target location.

3.3. Communications

Two UAVs exchange information when they are in vicinity. The UAV network is represented by a set of nodes $\mathcal{N}_u = \{1, 2, \ldots, N_u\}$. The set of edges of the network $\mathcal{E}_k \subset \mathcal{N}_u \times \mathcal{N}_u$ describes the connectivity at time k. An undirected graph $\mathcal{G}_k = (\mathcal{N}_u, \mathcal{E}_k)$ summarizes the communication topology of the fleet at time k. $\mathcal{N}_{i,k} = \{j \in \mathcal{N}_u | (i,j) \in \mathcal{E}_k,\ i \neq j\}$ is the set of neighbors connected to UAV i at time k. UAVs i and j exchange information without error when $(i,j) \in \mathcal{E}_k$, and they are unable to communicate when $(i,j) \notin \mathcal{E}_k$. The edges of the network at time k depend on some condition c. One has

$$c\left(\mathbf{x}^u_{i,k}, \mathbf{x}^u_{\ell,k}\right) \geqslant 0 \Rightarrow (i,j) \in \mathcal{E}_k. \tag{9}$$

3.4. Estimates

$\mathbb{I}_{i,k}$ gathers the information available to UAV i up to time k. From $\mathbb{I}_{i,k}$, UAV i is able to evaluate $\mathcal{L}_{i,k}$, the *list* of indices of true targets already detected and identified or which presence has been signaled by an other UAV of the fleet to UAV i. $\mathbb{I}_{i,k}$ is used to evaluate a list of target *set estimates* $\mathcal{X}_{i,k} = \{\mathbb{X}_{i,j,k}\}_{j \in \mathcal{L}_{i,k}}$ and $\mathbb{X}^U_{i,k}$. $\mathbb{X}_{i,j,k}$ contains all possible values of the state of the identified target j that are consistent with the information available to UAV i at time k. It is possible that $\mathbb{X}_{i,j,k}$ does not contain the actual values of $\mathbf{x}^t_{j,k}$ due to misidentification of false targets. $\mathbb{X}^U_{i,k}$ contains the union of all possible values of $\mathbf{x}^t_{j,k}$ and $\mathbf{x}^f_{\ell,k}$ of all detected targets still to be identified. Finally, UAV i also maintains a set $\overline{\mathbb{X}}_{i,k}$ containing the possible state values of true targets not yet detected.

3.5. Estimation uncertainty

Consider UAV i and assume that at time k, $\mathbb{X}^U_{i,k}$ and $\overline{\mathbb{X}}_{i,k}$ are empty and that set estimates $\mathbb{X}_{i,j,k}$ are available for all $j \in \mathcal{J}^t$. Then, $\mathbf{x}^t_{j,k} \in \mathbb{X}_{i,j,k}$ and the estimation uncertainty for the state of target j may be defined as $\phi(\mathbb{X}_{i,j,k})$, where $\phi(\mathbb{X})$ represents some measure of the set $\mathbb{X}$. When $\mathbb{X}^U_{i,k}$ or $\overline{\mathbb{X}}_{i,k}$ are not empty, due to the presence of decoys, one has not necessarily $\mathbf{x}^t_{j,k} \in \mathbb{X}_{i,j,k}$ and the estimation uncertainty for the state of target j has to account for $\mathbb{X}^U_{i,k}$ and $\overline{\mathbb{X}}_{i,k}$ (which both may contain $\mathbf{x}^t_{j,k}$) and may be defined as $\Phi_j(\mathcal{X}_{i,k}, \mathbb{X}^U_{i,k}, \overline{\mathbb{X}}_{i,k}) = \phi(\mathbb{X}_{i,j,k} \cup \mathbb{X}^U_{i,k} \cup \overline{\mathbb{X}}_{i,k})$. The estimation

uncertainty for target j is the measure of the union of the sets where target j may be.

The target state estimation uncertainty at time k for UAV i accounts for all sets in which the targets may be, *i.e.* ,

$$\Phi\left(\mathcal{X}_{i,k}, \mathbb{X}^{\mathrm{U}}_{i,k}, \overline{\mathbb{X}}_{i,k}\right) = \phi\left(\left(\bigcup_{\mathbb{X}_{i,j,k}\in\mathcal{X}_{i,k}} \mathbb{X}_{i,j,k}\right) \cup \mathbb{X}^{\mathrm{U}}_{i,k} \cup \overline{\mathbb{X}}_{i,k}\right). \tag{10}$$

When $\mathcal{X}_{i,k} = \emptyset$, (10) boils down to $\Phi(\mathcal{X}_{i,k}, \mathbb{X}^{\mathrm{U}}_{i,k}, \overline{\mathbb{X}}_{i,k}) = \phi(\mathbb{X}^{\mathrm{U}}_{i,k} \cup \overline{\mathbb{X}}_{i,k})$. Finally, the average estimation uncertainty among all UAVs at time k is

$$\overline{\Phi}_k = \frac{1}{N_{\mathrm{u}}} \sum_{i=1}^{N_{\mathrm{u}}} \Phi\left(\mathcal{X}_{i,k}, \mathbb{X}^{\mathrm{U}}_{i,k}, \overline{\mathbb{X}}_{i,k}\right). \tag{11}$$

The aim of this paper is to evaluate a sequence of control inputs for each UAV so as to minimize the estimation uncertainty $\overline{\Phi}_k$ as fast as possible. This requires first to be able to determine the evolution of the various set estimates managed by UAVs, as detailed in Section 4. A distributed control design strategy is then presented in Section 5.

4. Evolution of set estimates for a given UAV

This section describes the evolution with time of the sets $\mathcal{L}_{i,k}$, $\mathcal{X}_{i,k}$, $\mathbb{X}^{\mathrm{U}}_{i,k}$, and $\overline{\mathbb{X}}_{i,k}$ managed by a given UAV i. The UAVs evaluate the set estimates considering a generalization of the nonlinear recursive set-membership state estimator introduced in Kieffer, Jaulin, and Walter (2002). Similar to the classical Kalman filter, it alternates prediction and correction steps, the latter being based on measurements and communication. One has $\mathcal{L}_{i,0} = \emptyset$, $\mathcal{X}_{i,0} = \emptyset$, $\mathbb{X}^{\mathrm{U}}_{i,0} = \emptyset$ and $\overline{\mathbb{X}}_{i,0} = \mathbb{X}_0$ for $i = 1, \ldots, N_{\mathrm{u}}$ for the initialization at time $k = 0$.

4.1. Prediction step

UAV i has access to $\mathcal{L}_{i,k}$, $\mathcal{X}_{i,k}$, $\mathbb{X}^{\mathrm{U}}_{i,k}$, and $\overline{\mathbb{X}}_{i,k}$ at time k. One is unable to predict whether UAV i will detect new targets at time $k+1$, thus the predicted list of detected targets is

$$\mathcal{L}_{i,k+1|k} = \mathcal{L}_{i,k}, \tag{12}$$

For each target in $\mathcal{L}_{i,k+1|k}$, one is able to predict the set of possible future state values at time $k+1$, *i.e*, the set of all target state values that are consistent with $\mathbb{X}_{i,j,k}$, with the dynamics (2), and the bounded state perturbation

$$\begin{aligned}\mathbb{X}_{i,j,k+1|k} &= \left\{\mathbf{f}^{\mathrm{t}}_k(\mathbf{x},\mathbf{v}) \mid \mathbf{x}\in\mathbb{X}_{i,j,k}, \mathbf{v}\in[\mathbf{v}_k]\right\} \cap \mathbb{X}_0 \\ &= \mathbf{f}^{\mathrm{t}}_k\left(\mathbb{X}_{i,j,k}, [\mathbf{v}_k]\right) \cap \mathbb{X}_0.\end{aligned} \tag{13}$$

One computes the intersection with $\mathbb{X}_0$ since targets are assumed not to leave the area of interest. The update of the sets $\mathbb{X}^{\mathrm{U}}_{i,k+1|k}$ and $\overline{\mathbb{X}}_{i,k+1|k}$ is obtained in the same manner since all true targets evolve according to the same dynamics (2), $\mathbb{X}^{\mathrm{U}}_{i,k+1|k}$ is evaluated as

$$\begin{aligned}\mathbb{X}^{\mathrm{U}}_{i,k+1|k} &= \left\{\mathbf{f}^{\mathrm{t}}_k(\mathbf{x},\mathbf{v}) \mid \mathbf{x}\in\mathbb{X}^{\mathrm{U}}_{i,k}, \mathbf{v}\in[\mathbf{v}_k]\right\} \cap \mathbb{X}_0 \\ &= \mathbf{f}^{\mathrm{t}}_k\left(\mathbb{X}^{\mathrm{U}}_{i,k}, [\mathbf{v}_k]\right) \cap \mathbb{X}_0,\end{aligned} \tag{14}$$

and $\overline{\mathbb{X}}_{i,k+1|k}$ as

$$\begin{aligned}\overline{\mathbb{X}}_{i,k+1|k} &= \left\{\mathbf{f}^{\mathrm{t}}_k(\mathbf{x},\mathbf{v}) \mid \mathbf{x}\in\overline{\mathbb{X}}_{i,k}, \mathbf{v}\in[\mathbf{v}_k]\right\} \cap \mathbb{X}_0 \\ &= \left\{\mathbf{f}^{\mathrm{t}}_k\left(\overline{\mathbb{X}}_{i,k}, [\mathbf{v}_k]\right)\right\} \cap \mathbb{X}_0.\end{aligned} \tag{15}$$

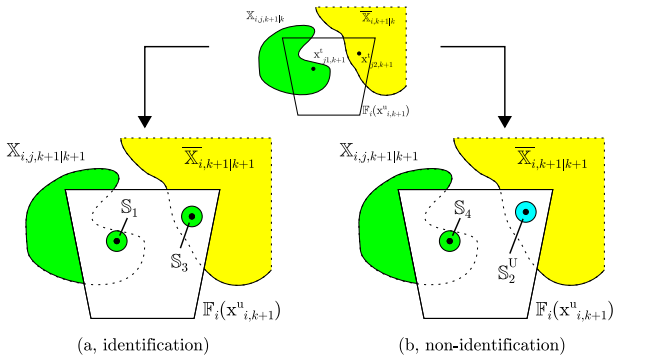

(a, identification) (b, non-identification)

Fig. 4. Correction from measurement I: set estimates $\mathbb{X}_{i,j,k+1|k}$ (in green) and $\overline{\mathbb{X}}_{i,k+1|k}$ (in yellow) before correction from measurement (top). Targets were detected and identified (a), the set estimates (in green) inside $\mathbb{F}_i\left(\mathbf{x}^{\mathrm{u}}_{i,k+1}\right)$ are $\mathbb{S}_1$ and $\mathbb{S}_3$. Targets were detected but not identified (b), the set estimate (in green) inside $\mathbb{F}_i\left(\mathbf{x}^{\mathrm{u}}_{i,k+1}\right)$ is $\mathbb{S}_4$. The set estimate (in cyan) inside $\mathbb{F}_i\left(\mathbf{x}^{\mathrm{u}}_{i,k+1}\right)$ is $\mathbb{S}^{\mathrm{U}}_2$.

4.2. Correction step from measurements

UAV i obtains measurement $\mathbf{y}^{\mathrm{I}}_{i,j,k+1}$ for identified targets $j \in \mathcal{D}^{\mathrm{I}}_{i,k+1}$ and measurement $\mathbf{y}^{\mathrm{U}}_{i,m,k+1}$ for unidentified targets $m \in \mathcal{D}^{\mathrm{U}}_{i,k+1}$ after processing the information in $\mathbb{F}_i\left(\mathbf{x}^{\mathrm{u}}_{i,k+1}\right)$ at time $k+1$. Consequently,

$$\begin{aligned}\mathbb{I}_{i,k+1|k+1} = \mathbb{I}_{i,k} \cup \Big\{ &\mathcal{D}^{\mathrm{I}}_{i,k+1}, \left\{\mathbf{y}^{\mathrm{I}}_{i,j,k+1}\right\}_{j\in\mathcal{D}^{\mathrm{I}}_{i,k+1}}, \\ &\mathcal{D}^{\mathrm{U}}_{i,k+1}, \left\{\mathbf{y}^{\mathrm{U}}_{i,m,k+1}\right\}_{m\in\mathcal{D}^{\mathrm{U}}_{i,k+1}} \Big\}.\end{aligned} \tag{16}$$

4.2.1. Updating the set of identified targets

One has to consider different cases to determine the updated set $\mathbb{X}_{i,j,k+1|k+1}$ from $\mathbb{X}_{i,j,k+1|k}$ for an identified target $j \in \mathcal{L}_{i,k+1|k+1}$, where $\mathcal{L}_{i,k+1|k+1} = \mathcal{L}_{i,k+1|k} \cup \mathcal{D}^{\mathrm{I}}_{i,k+1}$.

Accounting for measurements of identified targets

When $j \in \mathcal{D}^{\mathrm{I}}_{i,k+1}$, a measurement $\mathbf{y}^{\mathrm{I}}_{i,j,k+1}$ is available and four cases have to be considered.

If $\mathbb{X}_{i,j,k+1|k} \cap \mathbb{F}_i(\mathbf{x}^{\mathrm{u}}_{i,k+1}) \neq \emptyset$, then $\mathbf{y}^{\mathrm{I}}_{i,j,k+1}$ may correspond to a previously detected and identified target j that is observed again. Under that hypothesis, the set of all state values $\mathbf{x}$ consistent with $\mathbb{X}_{i,j,k+1|k}$, $\mathbf{y}^{\mathrm{I}}_{i,j,k+1}$, the measurement equations (5), and the measurement noise bound $[\mathbf{w}_{i,k+1}]$ is

$$\begin{aligned}\mathbb{S}_1 = \big\{&\mathbf{x}\in\mathbb{X}_{i,j,k+1|k} \mid \\ &\mathbf{h}_i\left(\mathbf{x}^{\mathrm{u}}_{i,k+1}, \mathbf{x}\right) \in \mathbf{y}^{\mathrm{I}}_{i,j,k+1} - [\mathbf{w}_{i,k+1}]\big\}.\end{aligned} \tag{17}$$

Fig. 4(a) illustrates the case where the set $\mathbb{S}_1 \neq \emptyset$.

If $\mathbb{X}^{\mathrm{U}}_{i,k+1|k} \cap \mathbb{F}_i(\mathbf{x}^{\mathrm{u}}_{i,k+1}) \neq \emptyset$, then $\mathbf{y}^{\mathrm{I}}_{i,j,k+1}$ may correspond to the true target j or to a false target ℓ, such that $J(\ell) = j$, which was only detected at k and (mis-)identified at time $k+1$. Under that hypothesis, the set of all state values $\mathbf{x}$ consistent with $\mathbb{X}^{\mathrm{U}}_{i,k+1|k}$, $\mathbf{y}^{\mathrm{I}}_{i,j,k+1}$, the measurement equations (5), and the measurement noise bound $[\mathbf{w}_{i,k+1}]$ is

$$\begin{aligned}\mathbb{S}_2 = \big\{&\mathbf{x}\in\mathbb{X}^{\mathrm{U}}_{i,k+1|k} \mid \\ &\mathbf{h}_i\left(\mathbf{x}^{\mathrm{u}}_{i,k+1}, \mathbf{x}\right) \in \mathbf{y}^{\mathrm{I}}_{i,j,k+1} - [\mathbf{w}_{i,k+1}]\big\}.\end{aligned} \tag{18}$$

Fig. 5(a) illustrates the case where $\mathbb{S}_2 \neq \emptyset$.

If $\overline{\mathbb{X}}_{i,k+1|k} \cap \mathbb{F}_i(\mathbf{x}^{\mathrm{u}}_{i,k+1}) \neq \emptyset$, then $\mathbf{y}^{\mathrm{I}}_{i,j,k+1}$ may correspond to a target in $\overline{\mathbb{X}}_{i,k+1|k} \cap \mathbb{F}_i(\mathbf{x}^{\mathrm{u}}_{i,k+1})$. This target may either be the true target j or a misidentified false target ℓ such that $J(\ell) = j$. The set of all state values $\mathbf{x}$ consistent with $\overline{\mathbb{X}}_{i,k+1|k}$, $\mathbf{y}^{\mathrm{I}}_{i,j,k+1}$, the

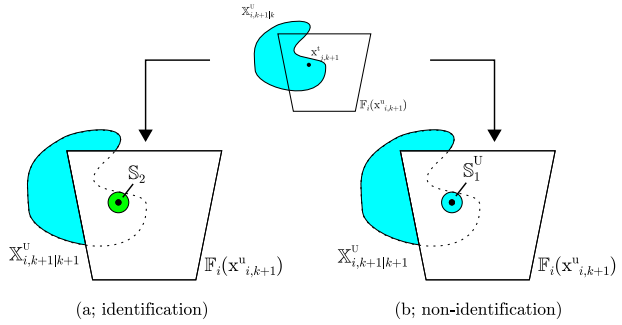

Fig. 5. Correction from measurement II: detection of a target inside $\mathbb{X}^{\mathrm{U}}_{i,k+1|k}$ (in cyan in the top subfigure): (a) a target is detected and identified as target j (possible mis-identification for a false target), the set estimate (in green) inside $\mathbb{F}_i\left(\mathbf{x}^{\mathrm{u}}_{i,k+1}\right)$ is $\mathbb{S}_2$; (b) the target is detected but not identified, the set estimate (in cyan) inside $\mathbb{F}_i\left(\mathbf{x}^{\mathrm{u}}_{i,k+1}\right)$ is $\mathbb{S}^{\mathrm{U}}_1$.

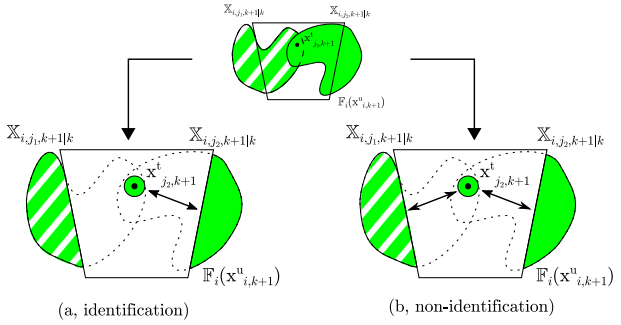

Fig. 6. Correction from measurement III: detection of a target inside the intersection of different target set estimates (green and striped green). The target was detected and identified (a), the set estimate (in green) inside $\mathbb{F}_i\left(\mathbf{x}^{\mathrm{u}}_{i,k+1}\right)$ is $\mathbb{S}_1$. The measurement can be linked to target j_2. The target was detected but not identified (b), the set estimate (in green) inside $\mathbb{F}_i\left(\mathbf{x}^{\mathrm{u}}_{i,k+1}\right)$ is $\mathbb{S}_4$. The measurement $\mathbf{y}^{\mathrm{U}}_{i,m,k+1}$ of state $\mathbf{x}^{\mathrm{t}}_{j_2,k+1}$ has to be considered for the estimates of j_1 and j_2 (green and striped green). (For interpretation of the references to colour in this figure legend, the reader is referred to the web version of this article.)

measurement equations (5), and the measurement noise bound $\left[\mathbf{w}_{i,k+1}\right]$ is

$$\mathbb{S}_3 = \left\{\mathbf{x} \in \overline{\mathbb{X}}_{i,k+1|k} \mid \mathbf{h}_i\left(\mathbf{x}^{\mathrm{u}}_{i,k+1}, \mathbf{x}\right) \in \mathbf{y}^{\mathrm{I}}_{i,j,k+1} - \left[\mathbf{w}_{i,k+1}\right]\right\}. \tag{19}$$

Fig. 4(a) illustrates the case where the set $\mathbb{S}_3 \neq \emptyset$.

Finally, if

$$\left(\mathbb{X}_{i,j,k+1|k} \cup \mathbb{X}^{\mathrm{U}}_{i,k+1|k} \cup \overline{\mathbb{X}}_{i,k+1|k}\right) \cap \mathbb{F}_i\left(\mathbf{x}^{\mathrm{u}}_{i,k+1}\right) = \emptyset,$$

then the measurement $\mathbf{y}^{\mathrm{I}}_{i,j,k+1}$ is necessarily due to a false target mis-identified with j, since $\mathbf{x}^{\mathrm{t}}_{j,k+1}$ is necessarily in $\mathbb{X}_{i,j,k+1|k} \cup \mathbb{X}^{\mathrm{U}}_{i,k+1|k} \cup \overline{\mathbb{X}}_{i,k+1|k}$.

Accounting for measurements of unidentified targets

When $j \in \mathcal{L}_{i,k+1|k}$ and $\mathcal{D}^{\mathrm{U}}_{i,k+1} \neq \emptyset$, we have to consider the case that one of the measurements $\mathbf{y}^{\mathrm{U}}_{i,m,k+1}$, $m \in \mathcal{D}^{\mathrm{U}}_{i,k+1}$, may be due to the detection of the true target j. Under that hypothesis, the set of all state values $\mathbf{x}$ consistent with $\mathbb{X}_{i,j,k+1|k}$, $\mathbf{y}^{\mathrm{U}}_{i,m,k+1}$, $m \in \mathcal{D}^{\mathrm{U}}_{i,k+1}$, the measurement equations (6), and the measurement noise bound $\left[\mathbf{w}_{i,k+1}\right]$ is

$$\mathbb{S}_4 = \bigcup_{m \in \mathcal{D}^{\mathrm{U}}_{i,k+1}} \left\{\mathbf{x} \in \mathbb{X}_{i,j,k+1|k} \mid \mathbf{h}_i\left(\mathbf{x}^{\mathrm{u}}_{i,k+1}, \mathbf{x}\right) \in \mathbf{y}^{\mathrm{U}}_{i,m,k+1} - \left[\mathbf{w}_{i,k+1}\right]\right\}. \tag{20}$$

Fig. 4(b) shows a case where $\mathbb{S}_4$ is not empty. $\mathbb{S}_4$ leads to situations where the measurements might be used several times for the set estimates of different targets. This is illustrated in Fig. 6(b). The observed target lays inside the intersection of two set estimates. The measurement has to be considered for both estimates if the target is not identified.

The sets $\mathbb{S}_1$ to $\mathbb{S}_4$ account for various hypotheses related to the obtained measurements which may be due to the true target j or to a false target misidentified with j. Additionally, one has to account for the fact that non-detection does not occur and that all information in $\mathbb{F}_i(\mathbf{x}^{\mathrm{u}}_{i,k})$ has been processed. Therefore, $\mathbf{x}^{\mathrm{t}}_{j,k+1} \notin \mathbb{F}_i(\mathbf{x}^{\mathrm{u}}_{i,k+1}) \setminus (\mathbb{S}_1 \cup \mathbb{S}_2 \cup \mathbb{S}_3 \cup \mathbb{S}_4)$. Introducing,

$$\mathbb{S}_5 = \mathbb{X}_{i,j,k+1|k} \setminus \mathbb{F}_i\left(\mathbf{x}^{\mathrm{u}}_{i,k+1}\right), \tag{21}$$

the updated set estimate accounting for all hypotheses, is then

$$\mathbb{X}_{i,j,k+1|k+1} = \mathbb{S}_1 \cup \mathbb{S}_2 \cup \mathbb{S}_3 \cup \mathbb{S}_4 \cup \mathbb{S}_5. \tag{22}$$

Some of the sets $\mathbb{S}_1, \ldots, \mathbb{S}_5$ may be empty.

When $j \notin \mathcal{L}_{i,k+1|k}$ and $j \in \mathcal{D}^{\mathrm{I}}_{i,k+1}$, the true target j or a false target misidentified with j is detected and identified for the first time. The set estimate (22) in that case boils down to

$$\mathbb{X}_{i,j,k+1|k+1} = \mathbb{S}_2 \cup \mathbb{S}_3. \tag{23}$$

4.2.2. Updating the set of unidentified targets

One has to consider different cases to determine the updated set $\mathbb{X}^{\mathrm{U}}_{i,k+1|k+1}$ from $\mathbb{X}^{\mathrm{U}}_{i,k+1|k}$ for an unidentified target using $\mathbf{y}^{\mathrm{U}}_{i,m,k+1}$, $m \in \mathcal{D}^{\mathrm{U}}_{i,k+1}$ obtained after processing the information in $\mathbb{F}_i(\mathbf{x}^{\mathrm{u}}_{i,k+1})$ at time $k+1$.

An unidentified target may be detected again inside the set estimate of unidentified targets $\mathbb{X}^{\mathrm{U}}{}_{i,k+1|k}$. This hypothesis is similar to that considered in (17), and one gets

$$\mathbb{S}^{\mathrm{U}}_1 = \bigcup_{m \in \mathcal{D}^{\mathrm{U}}_{i,k+1}} \left\{\mathbf{x} \in \mathbb{X}^{\mathrm{U}}_{i,k+1|k} \mid \mathbf{h}_{k+1}\left(\mathbf{x}^{\mathrm{u}}_{i,k+1}, \mathbf{x}\right) \in \mathbf{y}^{\mathrm{U}}_{i,m,k+1} - [\mathbf{w}_{k+1}]\right\}. \tag{24}$$

Alternatively, an unidentified target may be detected for the first time in the unexplored set $\overline{\mathbb{X}}_{i,k+1|k}$. This hypothesis is similar to that leading to (19), and one gets

$$\mathbb{S}^{\mathrm{U}}_2 = \bigcup_{m \in \mathcal{D}^{\mathrm{U}}_{i,k+1}} \left\{\mathbf{x} \in \overline{\mathbb{X}}_{i,k+1|k} \mid \mathbf{h}_{k+1}\left(\mathbf{x}^{\mathrm{u}}_{i,k+1}, \mathbf{x}\right) \in \mathbf{y}^{\mathrm{U}}_{i,m,k+1} - [\mathbf{w}_{k+1}]\right\}. \tag{25}$$

Contrary to (19) and (17), $\mathbb{S}^{\mathrm{U}}_1$ and $\mathbb{S}^{\mathrm{U}}_2$ contain the union of the set estimates associated to all detected targets in $m \in \mathcal{D}^{\mathrm{U}}_{i,k+1}$. Figs. 4(b) and 5(b) illustrate situations where $\mathbb{S}^{\mathrm{U}}_1 \subset \mathbb{F}_i(\mathbf{x}^{\mathrm{u}}_{i,k+1})$ and $\mathbb{S}^{\mathrm{U}}_2 \subset \mathbb{F}_i(\mathbf{x}^{\mathrm{u}}_{i,k+1})$ (both in cyan) are not empty.

Again, one has to account for the fact that non-detection does not occur and that all information in $\mathbb{F}_i(\mathbf{x}^{\mathrm{u}}_{i,k})$ has been processed. Therefore, $\mathbf{x}^{\mathrm{t}}_{j,k+1} \notin \mathbb{F}_i(\mathbf{x}^{\mathrm{u}}_{i,k+1}) \setminus \left(\mathbb{S}^{\mathrm{U}}_1 \cup \mathbb{S}^{\mathrm{U}}_2\right)$. Introducing,

$$\mathbb{S}^{\mathrm{U}}_3 = \mathbb{X}^{\mathrm{U}}{}_{i,k+1|k} \setminus \mathbb{F}_i\left(\mathbf{x}^{\mathrm{u}}_{i,k+1}\right), \tag{26}$$

the updated set estimate $\mathbb{X}^{\mathrm{U}}{}_{i,k+1|k+1}$ accounting for all hypotheses, is then

$$\mathbb{X}^{\mathrm{U}}{}_{i,k+1|k+1} = \mathbb{S}^{\mathrm{U}}_1 \cup \mathbb{S}^{\mathrm{U}}_2 \cup \mathbb{S}^{\mathrm{U}}_3. \tag{27}$$

When all measurements from $\mathbb{F}_i(\mathbf{x}^{\mathrm{u}}_{i,k+1})$ are processed, the unexplored set $\overline{\mathbb{X}}_{i,k+1|k}$ can be updated as

$$\overline{\mathbb{X}}_{i,k+1|k+1} = \overline{\mathbb{X}}_{i,k+1|k} \setminus \mathbb{F}_i\left(\mathbf{x}^{\mathrm{u}}_{i,k+1}\right). \tag{28}$$

Finally, one has to remove all targets j from the list of already detected and identified targets whose set $\mathbb{X}_{i,j,k+1|k+1}$ is empty

$$\mathcal{L}_{i,k+1|k+1} = \left\{ j \in \mathcal{L}_{i,k+1|k} \mid \mathbb{X}_{i,j,k+1|k+1} \neq \emptyset \right\}. \tag{29}$$

This case may appear if, for example, false target ℓ was detected and misidentified as a true target $j \in \mathcal{T}^{\mathrm{t}}$ at time k, and new observations lead to the identification as false target at time $k+1$.

4.3. Correction step from communications

UAV i sends the sets $\mathcal{L}_{i,k+1|k+1}$, $\mathbb{X}^{\mathrm{U}}{}_{i,k+1|k+1}$, $\overline{\mathbb{X}}_{i,k+1|k+1}$, and $\mathcal{X}_{i,k+1|k+1} = \left\{ \mathbb{X}_{i,j,k+1|k+1} \right\}_{j \in \mathcal{L}_{i,k+1|k+1}}$, to its neighbors $\ell \in \mathcal{N}_{i,k+1}$, and it receives the corresponding sets from its neighbors at the end of time step $k+1$. The information available to UAV i is then

$$\begin{aligned} \mathbb{I}_{i,k+1} = & \mathbb{I}_{i,k+1|k+1} \bigcup_{\ell \in \mathcal{N}_{i,k+1}} \left\{ \mathcal{L}_{\ell,k+1|k+1}, \right. \\ & \left. \mathcal{X}_{\ell,k+1|k+1}, \mathbb{X}^{\mathrm{U}}{}_{\ell,k+1|k+1}, \overline{\mathbb{X}}_{\ell,k+1|k+1} \right\}. \end{aligned} \tag{30}$$

Accounting for the information exchanged with UAV i, the set of all targets which have been identified by UAV i or one of its neighbors up to time $k+1$ is then

$$\mathcal{L}^{+}_{i,k+1|k+1} = \bigcup_{\ell \in \mathcal{N}_{i,k+1} \cup \{i\}} \mathcal{L}_{\ell,k+1|k+1}. \tag{31}$$

Then, for each $j \in \mathcal{L}^{+}_{i,k+1|k+1}$, the set of neighbors $\mathcal{N}_{i,k+1}$ of UAV i can be partitioned into two subsets. The subset $\mathcal{N}^{j}_{i,k+1}$ of the neighbors who *believe* that they have detected target j up to time $k+1$ and the subset $\overline{\mathcal{N}}^{j}_{i,k+1}$ of neighbors who are *sure* that they have *not* detected target j up to time $k+1$.

To further fuse the information available to UAV i before and after communication, for all $j \in \mathcal{L}^{+}_{i,k+1|k+1}$, we introduce

$$\begin{aligned} \widetilde{\mathbb{X}}_{i,j,k+1|k+1} = & \mathbb{X}_0 \setminus \left(\mathbb{X}_{i,j,k+1|k+1} \cup \right. \\ & \left. \mathbb{X}^{\mathrm{U}}_{i,k+1|k+1} \cup \overline{\mathbb{X}}_{i,k+1|k+1} \right) \end{aligned} \tag{32}$$

as the set *proved not to contain* the state of target j, *i.e.*, $\mathbf{x}^{\mathrm{t}}_{j,k+1} \notin \widetilde{\mathbb{X}}_{i,j,k+1|k+1}$, where, by convention, $\mathbb{X}_{i,j,k+1|k+1} = \emptyset$ when $j \notin \mathcal{L}_{i,k+1}$. We also introduce

$$\widetilde{\mathbb{X}}^{\mathrm{U}}_{i,k+1|k+1} = \mathbb{X}_0 \setminus \left(\mathbb{X}^{\mathrm{U}}_{i,k+1|k+1} \cup \overline{\mathbb{X}}_{i,k+1|k+1} \right) \tag{33}$$

the set *proved not to contain* the state of any unidentified target.

Considering UAV i, for any target $j \in \mathcal{L}_{i,k+1|k+1}$, one knows that either $\mathbf{x}^{\mathrm{t}}_{j,k+1} \in \mathbb{X}_{i,j,k+1|k+1}$, or $\mathbf{x}^{\mathrm{t}}_{j,k+1} \in \mathbb{X}^{\mathrm{U}}_{i,k+1|k+1}$, or $\mathbf{x}^{\mathrm{t}}_{j,k+1} \in \overline{\mathbb{X}}_{i,k+1|k+1}$. Moreover, one has $\mathbf{x}^{\mathrm{t}}_{j,k+1} \notin \widetilde{\mathbb{X}}_{i,j,k+1|k+1}$. Similarly, considering UAV $\ell \in \mathcal{N}^{j}_{i,k+1}$, *i.e.*, such that $j \in \mathcal{L}_{\ell,k+1|k+1}$, one has either $\mathbf{x}^{\mathrm{t}}_{j,k+1} \in \mathbb{X}_{\ell,j,k+1|k+1}$, or $\mathbf{x}^{\mathrm{t}}_{j,k+1} \in \mathbb{X}^{\mathrm{U}}_{\ell,k+1|k+1}$, or $\mathbf{x}^{\mathrm{t}}_{j,k+1} \in \overline{\mathbb{X}}_{\ell,k+1|k+1}$. Moreover, one knows that $\mathbf{x}^{\mathrm{t}}_{j,k+1} \notin \widetilde{\mathbb{X}}_{\ell,j,k+1|k+1}$. Consequently, for UAV i and any target $j \in \mathcal{L}^{+}_{i,k+1|k+1}$, $\mathbb{X}_{i,j,k+1}$ is evaluated as the union of all possible state values accounting for the measurements of the identified target j, deprived of the union of all sets which have been proved not to contain target j at time $k+1$, *i.e.*,

$$\mathbb{X}_{i,j,k+1} = \bigcup_{\ell \in \mathcal{N}^{j}_{i,k+1} \cup \{i\}} \mathbb{X}_{\ell,j,k+1|k+1} \setminus \bigcup_{\ell \in \mathcal{N}_{i,k+1} \cup \{i\}} \widetilde{\mathbb{X}}_{\ell,j,k+1|k+1}. \tag{34}$$

The list $\mathcal{L}_{i,k+1|k+1}$ of all targets j known to UAV i has to be updated from $\mathcal{L}^{+}_{i,k+1|k+1}$ accounting only for estimates $\mathbb{X}_{i,j,k+1}$ which are not empty

$$\mathcal{L}_{i,k+1} = \left\{ j \in \mathcal{L}^{+}_{i,k+1|k+1} \mid \mathbb{X}_{i,j,k+1} \neq \emptyset \right\}. \tag{35}$$

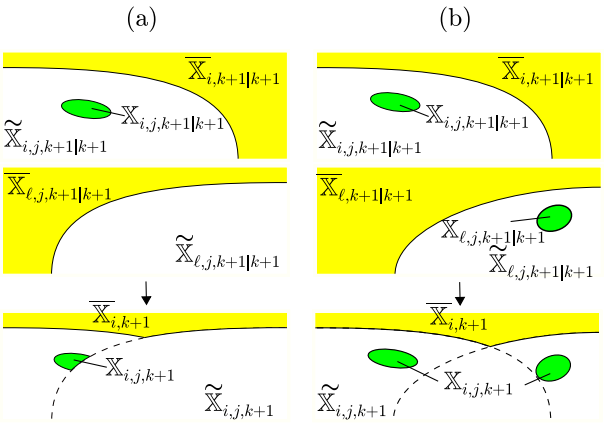

Fig. 7. Set estimates evaluated by UAV i and ℓ before communication (two top subfigures of each column) and after communication and update (bottom subfigures); (a) $\mathbb{X}_{i,j,k+1}$ is smaller than $\mathbb{X}_{i,j,k+1|k+1}$ since some subsets of $\mathbb{X}_{i,j,k+1|k+1}$ have been proved by UAV ℓ not to contain a target; (b) $\mathbb{X}_{i,j,k+1}$ is larger than $\mathbb{X}_{i,j,k+1|k+1}$, since UAV i has to account for the two different hypotheses on the state estimate of target j.

The update of $\mathbb{X}^{\mathrm{U}}_{i,k+1|k+1}$ is evaluated as the union of the set estimates of unidentified targets reduced by the space which is proved not to contain any unidentified target, *i.e.*,

$$\mathbb{X}^{\mathrm{U}}_{i,k+1} = \bigcup_{\ell \in \mathcal{N}_{i,k+1} \cup \{i\}} \mathbb{X}^{\mathrm{U}}_{\ell,k+1|k+1} \setminus \bigcup_{\ell \in \mathcal{N}_{i,k+1} \cup \{i\}} \widetilde{\mathbb{X}}^{\mathrm{U}}_{\ell,k+1|k+1}. \tag{36}$$

Finally, the update of $\overline{\mathbb{X}}_{i,k+1|k+1}$ is the intersection of the unexplored space of UAV i and that of its neighbors

$$\overline{\mathbb{X}}_{i,k+1} = \bigcap_{\ell \in \mathcal{N}_{i,k+1} \cup \{i\}} \overline{\mathbb{X}}_{\ell,k+1|k+1}. \tag{37}$$

Fig. 7 illustrates the sets resulting from (34) and (37) for two cases. The size of $\mathbb{X}_{i,j,k+1}$ may be smaller than $\mathbb{X}_{i,j,k+1|k+1}$ as it is the case in Fig. 7(a), when some subsets of $\mathbb{X}_{i,j,k+1|k+1}$ have been proved by another UAV not to contain a target. It may also be larger, as is the case in Fig. 7(b), where UAV ℓ has obtained measurements leading to another hypothesis on the state estimate of target j. The evolution of $\mathbb{X}^{\mathrm{U}}_{i,k+1}$ from $\mathbb{X}^{\mathrm{U}}_{i,k+1|k+1}$ could be illustrated with similar figures. The size of $\overline{\mathbb{X}}_{i,k+1}$ is always reduced compared to that of $\overline{\mathbb{X}}_{i,k+1|k+1}$.

4.4. Algorithm

Algorithm 1, summarizes the prediction and correction steps from both measurements and communications.

4.5. Accounting for delayed information

In case of reception of delayed information from another UAV, the estimation technique has to be significantly updated. A solution similar to the state augmentation approach considered in Lu, Zhang, Wang, and Teo (2005) may be proposed in our set-membership estimation context. For that purpose, we assume that the UAVs have synchronized clocks, update their estimate periodically and synchronously, and that the transmitted data are properly time stamped. Moreover, only information with a delay δ less than or equal to $\overline{\delta}$ time steps are processed to limit computational complexity.

At time k, UAV i has to maintain the sets $\mathcal{L}_{i,k-\delta}$, $\mathcal{X}_{i,k-\delta}$, $\mathbb{X}^{\mathrm{U}}_{i,k-\delta}$, and $\overline{\mathbb{X}}_{i,k-\delta}$, $\delta = 0, \ldots, \overline{\delta}$ corresponding to the estimates at time k as well as the estimates at time $k-\delta$, $\delta = 1, \ldots, \overline{\delta}$. Assume that UAV i receives $\mathcal{L}_{\ell,k-\delta'}$, $\mathcal{X}_{\ell,k-\delta'}$, $\mathbb{X}^{\mathrm{U}}_{\ell,k-\delta'}$, and $\overline{\mathbb{X}}_{\ell,k-\delta'}$ from UAV $\ell \neq i$

Algorithm 1. Robust Cooperative Bounded-error Target Localization and Tracking

RoCoBoTLoT$\left(\mathcal{L}_{i,k}, \mathcal{X}_{i,k}, \overline{\mathbb{X}}_{i,k}\right)$

Input: $\mathcal{L}_{i,k}$, $\mathcal{X}_{i,k}$, $\mathbb{X}^{\mathrm{U}}_{i,k}$, and $\overline{\mathbb{X}}_{i,k}$
Output: $\mathcal{L}_{i,k+1}$, $\mathcal{X}_{i,k+1}$, $\mathbb{X}^{\mathrm{U}}_{i,k+1}$, and $\overline{\mathbb{X}}_{i,k+1}$
Prediction step
$\mathcal{L}_{i,k+1|k} = \mathcal{L}_{i,k}$
$\mathbb{X}_{i,j,k+1|k} = \mathbf{f}^{\mathrm{t}}_k\left(\mathbb{X}_{i,j,k}, [\mathbf{v}_k]\right) \cap \mathbb{X}_0$, for all $j \in \mathcal{L}_{i,k+1|k}$
$\mathbb{X}^{\mathrm{U}}_{i,k+1|k} = \mathbf{f}^{\mathrm{t}}_k\left(\mathbb{X}^{\mathrm{U}}_{i,k}, [\mathbf{v}_k]\right) \cap \mathbb{X}_0$
$\overline{\mathbb{X}}_{i,k+1|k} = \mathbf{f}^{\mathrm{t}}_k\left(\overline{\mathbb{X}}_{i,k}, [\mathbf{v}_k]\right) \cap \mathbb{X}_0$
Correction step from measurements
$\mathcal{L}^{+}_{i,k+1|k} = \mathcal{L}_{i,k+1|k} \cup \mathcal{D}^{\mathrm{I}}_{i,k}$
For all $j \in \mathcal{L}^{+}_{i,k+1|k}$
  $\mathbb{X}_{i,j,k+1|k+1}$ updated as in (22)
$\mathcal{L}_{i,k+1|k+1} = \left\{j \in \mathcal{L}^{+}_{i,k+1|k} \,|\, \mathbb{X}_{i,j,k+1|k+1} \neq \emptyset\right\}$
$\mathbb{X}^{\mathrm{U}}{}_{i,k+1|k+1}$ updated as in (27)
$\overline{\mathbb{X}}_{i,k+1|k+1} = \overline{\mathbb{X}}_{i,k+1|k} \setminus \mathbb{F}_i(\mathbf{x}^{\mathrm{u}}_{i,k+1})$
Correction step from communications
$\mathcal{L}^{+}_{i,k+1|k+1} = \bigcup_{\ell \in \mathcal{N}_{i,k+1} \cup \{i\}} \mathcal{L}_{\ell,k+1|k+1}$
For all $j \in \mathcal{L}^{+}_{i,k+1|k+1}$
$\mathbb{X}_{i,j,k+1} = \bigcup_{\ell \in \mathcal{N}^{j}_{i,k+1} \cup \{i\}} \mathbb{X}_{\ell,j,k+1|k+1} \setminus \bigcup_{\ell \in \mathcal{N}_{i,k+1} \cup \{i\}} \widetilde{\mathbb{X}}_{\ell,j,k+1|k+1}$
$\mathcal{L}_{i,k+1} = \left\{j \in \mathcal{L}^{+}_{i,k+1|k+1} \,|\, \mathbb{X}_{i,j,k+1} \neq \emptyset\right\}$
$\mathbb{X}^{\mathrm{U}}_{i,k+1} = \bigcup_{\ell \in \mathcal{N}^{j}_{i,k+1} \cup \{i\}} \mathbb{X}^{\mathrm{U}}_{\ell,k+1|k+1} \setminus \bigcup_{\ell \in \mathcal{N}_{i,k+1} \cup \{i\}} \widetilde{\mathbb{X}}^{\mathrm{U}}_{\ell,k+1|k+1}$
$\overline{\mathbb{X}}_{i,k+1} = \overline{\mathbb{X}}_{i,k+1|k+1} \bigcap_{\ell \in \mathcal{N}_{i,k+1} \cup \{i\}} \overline{\mathbb{X}}_{\ell,k+1|k+1}$

at time k, with $\delta' \in \left[0, \overline{\delta}\right]$. The sets $\mathcal{L}_{\ell,k-\delta'}$, $\mathcal{X}_{\ell,k-\delta'}$, $\mathbb{X}^{\mathrm{U}}_{\ell,k-\delta'}$, and $\overline{\mathbb{X}}_{\ell,k-\delta'}$ can be used to update $\mathcal{L}_{i,k-\delta'}$, $\mathcal{X}_{i,k-\delta'}$, $\mathbb{X}^{\mathrm{U}}_{i,k-\delta'}$, and $\overline{\mathbb{X}}_{i,k-\delta'}$ using the procedure described in Section 4.3. These updated sets can then be used by UAV i to further update $\mathcal{L}_{i,k-\delta}$, $\mathcal{X}_{i,k-\delta}$, $\mathbb{X}^{\mathrm{U}}_{i,k-\delta}$, and $\overline{\mathbb{X}}_{i,k-\delta}$, $\delta = \delta' - 1, \ldots, 0$. This is done for each value of δ using the prediction step described in Section 4.1 and the correction steps from communication described in Section 4.3.

Processing delayed measurements significantly increases the computational complexity, as it is also the case in the state augmentation approaches considered in Lu et al. (2005).

5. Cooperative control design

The aim of the control design for the fleet of UAVs is to decrease the estimation uncertainty as much as possible. To achieve this task, we will consider the problem of determining, at each time k and in a distributed way, the sequence of control inputs which minimizes the predicted estimation uncertainty (11) at time $k + h$

$$\overline{\Phi}_{k+h} = \frac{1}{N_{\mathrm{u}}} \sum_{i=1}^{N_{\mathrm{u}}} \Phi\left(\mathcal{X}_{i,k+h}, \mathbb{X}^{\mathrm{U}}_{i,k+h}, \overline{\mathbb{X}}_{i,k+h}\right), \tag{38}$$

where $h \geqslant 1$ is the considered prediction horizon. UAVs have no access to all the terms of (38), thus each UAV i, $i = 1, \ldots, N_{\mathrm{u}}$, will try to minimize the term $\Phi(\mathcal{X}_{i,k+h}, \mathbb{X}^{\mathrm{U}}_{i,k+h}, \overline{\mathbb{X}}_{i,k+h})$ given by (10).

We consider the distributed Model Predictive Control (MPC) formalism introduced, *e.g.,* in Camacho and Alba (2013) and Morari and Lee (1999) to predict the evolution of (10). In the proposed set-membership estimation context, some simplifications are introduced to do so. We will first consider an h-step ahead prediction ignoring communication between neighboring UAVs. Then the impact of communications will be taken into account in the Set-Membership Model Predictive Control (SM-MPC) approach.

5.1. Control input design ignoring future communications

When the communications in time steps $k+1, \ldots, k+h$ are ignored, the control inputs of each UAV can be designed independently. Obviously, the communications which have previously occurred are taken into account.

At time k, UAV i has access to $\mathcal{L}_{i,k}$, $\mathcal{X}_{i,k}$, $\mathbb{X}^{\mathrm{U}}_{i,k}$, and $\overline{\mathbb{X}}_{i,k}$. Using a prediction step described in Section 4.1, UAV i is able to evaluate $\mathcal{L}_{i,k+1|k} = \mathcal{L}_{i,k}$, $\mathbb{X}_{i,j,k+1|k}$, $j \in \mathcal{L}_{i,k}$, $\mathbb{X}^{\mathrm{U}}_{i,k+1|k}$, and $\overline{\mathbb{X}}_{i,k+1|k}$. Then, for a given control input $\mathbf{u}_{i,k}$, UAV i is able to get a predicted value $\mathbf{x}^{\mathrm{u,P}}_{i,k+1}$ of its state $\mathbf{x}^{\mathrm{u}}_{i,k+1}$ at time $k+1$ and to infer the corresponding field of view $\mathbb{F}_i(\mathbf{x}^{\mathrm{u,P}}_{i,k+1})$. Nevertheless, UAV i is unable to determine whether it will observe new or previously detected targets in $\mathbb{F}_i(\mathbf{x}^{\mathrm{u,P}}_{i,k+1})$. Consequently, in the update from measurement equations described in Section 4.2, only $\mathbb{S}_5$ in (21), $\mathbb{S}^{\mathrm{U}}_3$ in (26), and $\overline{\mathbb{X}}_{i,k+1|k+1}$ in (28) can be inferred accurately as follows

$$\mathbb{X}^{\mathrm{P}}_{i,j,k+1|k+1} = \mathbb{X}_{i,j,k+1|k} \setminus \mathbb{F}_i\left(\mathbf{x}^{\mathrm{u,P}}_{i,k+1}\right), j \in \mathcal{L}_{i,k} \tag{39}$$

$$\mathbb{X}^{\mathrm{U,P}}_{i,k+1|k+1} = \mathbb{X}^{\mathrm{U}}_{i,k+1|k} \setminus \mathbb{F}_i\left(\mathbf{x}^{\mathrm{u,P}}_{i,k+1}\right), \tag{40}$$

$$\overline{\mathbb{X}}^{\mathrm{P}}_{i,k+1|k+1} = \overline{\mathbb{X}}_{i,k+1|k} \setminus \mathbb{F}_i\left(\mathbf{x}^{\mathrm{u,P}}_{i,k+1}\right). \tag{41}$$

If $\mathbf{x}^{\mathrm{u}}_{i,k+1} = \mathbf{x}^{\mathrm{u,P}}_{i,k+1}$, then $\mathbb{X}^{\mathrm{P}}_{i,j,k+1|k+1} \subset \mathbb{X}_{i,j,k+1|k+1}$, $\mathbb{X}^{\mathrm{U,P}}_{i,k+1|k+1} \subset \mathbb{X}^{\mathrm{U}}_{i,k+1|k+1}$, and $\overline{\mathbb{X}}^{\mathrm{P}}_{i,k+1|k+1} = \overline{\mathbb{X}}_{i,k+1|k+1}$.

Using the previous approximations, a predicted estimation uncertainty for UAV i at time $k+1$ may be evaluated as

$$\Phi\left(\mathcal{X}^{\mathrm{P}}_{i,k+1|k+1}, \mathbb{X}^{\mathrm{U,P}}_{i,k+1|k+1}, \overline{\mathbb{X}}^{\mathrm{P}}_{i,k+1|k+1}\right) = \phi\left(\left(\bigcup_{j \in \mathcal{L}_{i,k}} \mathbb{X}^{\mathrm{P}}_{i,j,k+1|k+1}\right) \cup \mathbb{X}^{\mathrm{U,P}}_{i,k+1|k+1} \cup \overline{\mathbb{X}}^{\mathrm{P}}_{i,k+1|k+1}\right). \tag{42}$$

Despite the approximation performed in the evaluation of $\mathbb{X}^{\mathrm{P}}_{i,j,k+1|k+1}, j \in \mathcal{L}_{i,k}$ and $\mathbb{X}^{\mathrm{U,P}}_{i,k+1|k+1}$, the contribution of the missing part of these sets is usually negligible compared to that of $\overline{\mathbb{X}}^{\mathrm{P}}_{i,k+1|k+1}$ in the evaluation of Φ.

In order to compute (42) more efficiently, at time k, consider the set, known to UAV i,

$$\mathbb{X}^{\mathrm{A}}_{i,k} = \left(\bigcup_{j \in \mathcal{L}_{i,k}} \mathbb{X}_{i,j,k}\right) \cup \mathbb{X}^{\mathrm{U}}_{i,k} \cup \overline{\mathbb{X}}_{i,k}, \tag{43}$$

aggregating the states of all detected targets and the states of not yet detected targets. Exploiting the target dynamics (2) and the common bound on the state perturbation $[\mathbf{v}_k]$, the predicted value of $\mathbb{X}^{\mathrm{A}}_{i,k}$ in (43) at time $k+1$ is

$$\mathbb{X}^{\mathrm{A}}_{i,k+1|k} = \mathbf{f}^{\mathrm{t}}_k\left(\mathbb{X}^{\mathrm{A}}_{i,k}, [\mathbf{v}_k]\right) \cap \mathbb{X}_0. \tag{44}$$

Considering (13), (14), and (15), one observes that

$$\mathbb{X}^{\mathrm{A}}_{i,k+1|k} = \left(\bigcup_{j \in \mathcal{L}_{i,k}} \mathbb{X}_{i,j,k+1|k}\right) \cup \mathbb{X}^{\mathrm{U}}_{i,k+1|k} \cup \overline{\mathbb{X}}_{i,k+1|k}. \tag{45}$$

Now, introducing the corrected set at time $k+1$

$$\mathbb{X}^{\mathrm{A,P}}_{i,k+1|k+1} = \mathbb{X}^{\mathrm{A}}_{i,k+1|k} \setminus \mathbb{F}_i\left(\mathbf{x}^{\mathrm{u,P}}_{i,k+1}\right), \tag{46}$$

where the superscript $^{\mathrm{P}}$ indicates that this is a predicted value of $\mathbb{X}^{\mathrm{A}}_{i,k+1|k+1}$, relying on the various assumptions considered in the proposed SM-MPC approach. Combining (45) and (46), one easily

shows that

$$\mathbb{X}^{\mathrm{A,P}}_{i,k+1|k+1} = \left(\bigcup_{j\in\mathcal{L}_{i,k}} \mathbb{X}_{i,j,k+1|k} \cup \mathbb{X}^{\mathrm{U}}_{i,k+1|k} \cup \overline{\mathbb{X}}_{i,k+1|k} \right) \setminus \mathbb{F}_i\left(\mathbf{x}^{\mathrm{u,P}}_{i,k+1}\right) = \bigcup_{j\in\mathcal{L}_{i,k}} \mathbb{X}^{\mathrm{P}}_{i,j,k+1|k+1} \cup \mathbb{X}^{\mathrm{U,P}}_{i,k+1|k+1} \cup \overline{\mathbb{X}}^{\mathrm{P}}_{i,k+1|k+1}.$$

Introducing $\mathbb{X}^{\mathrm{A,P}}_{i,k+1} = \mathbb{X}^{\mathrm{A,P}}_{i,k+1|k+1}$, the predicted estimation uncertainty for UAV i at time $k+1$, provided by (42), is also given by $\phi\left(\mathbb{X}^{\mathrm{A,P}}_{i,k+1}\right)$. Consequently, considering $\mathbb{X}^{\mathrm{A}}_{i,k}$, instead of $\mathcal{X}_{i,k}$, $\mathbb{X}^{\mathrm{U}}_{i,k}$, and $\overline{\mathbb{X}}_{i,k}$ and applying the prediction step (44) and the correction step (46) to $\mathbb{X}^{\mathrm{A}}_{i,k}$ is sufficient to evaluate the predicted estimation uncertainty for UAV i at time $k+1$.

The previous approach may be applied iteratively on $\mathbb{X}^{\mathrm{A,P}}_{i,k+\kappa-1}$ to evaluate the impact of $\mathbf{u}_{i,k+\kappa}$, $\kappa = 1,\ldots,h-1$ on the predicted estimation uncertainty for UAV i at time $k+\kappa$, which provides $\mathbb{X}^{\mathrm{A,P}}_{i,k+h}$ when $\kappa = h-1$. Thus an estimate $\phi(\mathbb{X}^{\mathrm{A,P}}_{i,k+h}) = \Phi(\mathcal{X}^{\mathrm{P}}_{i,k+h}, \mathbb{X}^{\mathrm{U,P}}_{i,k+h}, \overline{\mathbb{X}}^{\mathrm{P}}_{i,k+h})$ of $\Phi(\mathcal{X}_{i,k+h}, \mathbb{X}^{\mathrm{U}}_{i,k+h}, \overline{\mathbb{X}}_{i,k+h})$ is deduced. Then UAV i may search the sequence of control inputs $\left(\mathbf{u}_{i,k},\ldots,\mathbf{u}_{i,k+h-1}\right)$ minimizing

$$J\left(\mathbf{u}_{i,k},\ldots,\mathbf{u}_{i,k+h-1}\right) = \phi\left(\mathbb{X}^{\mathrm{A,P}}_{i,k+h}\right) + \alpha d\left(\mathbf{x}^{\mathrm{u,P}}_{i,k+h}, \mathbb{X}^{\mathrm{A,P}}_{i,k+h}\right), \tag{47}$$

where $\mathbb{X}^{\mathrm{A,P}}_{i,k+h}$ and $\mathbf{x}^{\mathrm{u,P}}_{i,k+h}$ depend on $\left(\mathbf{u}_{i,k},\ldots,\mathbf{u}_{i,k+h-1}\right)$. In (47), $d(\mathbf{x},\mathbb{X})$ represents the Hausdorff distance between the vector $\mathbf{x}$ and the set $\mathbb{X}$. The first term of J represents the predicted estimation uncertainty for UAV i at time $k+h$. The second term is introduced to drive UAV i towards $\mathbb{X}^{\mathrm{A,P}}_{i,k+h}$. This is useful when the first term of the cost function remains constant, whatever the sequence of inputs $\left(\mathbf{u}_{i,k},\ldots,\mathbf{u}_{i,k+h-1}\right)$. The parameter α adjusts the importance of the second term.

5.2. Control input design accounting for communications

Assume that some UAVs in a subset $\mathcal{N}^{\mathrm{C}}_{i,k} \subset \mathcal{N}_{i,k}$ of neighbors of UAV i have already computed and transmitted their own control inputs $\left(\mathbf{u}_{\ell,k},\ldots,\mathbf{u}_{\ell,k+h-1}\right)$, $\ell \in \mathcal{N}^{\mathrm{C}}_{i,k}$, as well as their state value at time k. To evaluate its own sequence $\left(\mathbf{u}_{i,k},\ldots,\mathbf{u}_{i,k+h-1}\right)$ of control inputs, UAV i will now account for the information that will be provided via communications at the steps $k+\kappa$ by the agents in $\mathcal{N}^{\mathrm{C}}_{i,k+\kappa}$, $\kappa = 1,\ldots,h$. Nevertheless, some UAVs in $\mathcal{N}^{\mathrm{C}}_{i,k}$ may not be able to communicate with UAV i at some prediction steps $\kappa = 1,\ldots,h$. We have thus to predict for each κ, the set of UAVs with which UAV i will be able to communicate. For each UAV $\ell \in \mathcal{N}^{\mathrm{C}}_{i,k}$, consider the sequences of control inputs $\left(\mathbf{u}_{\ell,k},\ldots,\mathbf{u}_{\ell,k+h-1}\right)$ and $\left(\mathbf{u}_{i,k},\ldots,\mathbf{u}_{i,k+h-1}\right)$, as well as the states $\mathbf{x}^{\mathrm{u}}_{\ell,k}$ and $\mathbf{x}^{\mathrm{u}}_{i,k}$. UAV i can evaluate $\mathbf{x}^{\mathrm{u,P}}_{\ell,k+\kappa}$ and $\mathbf{x}^{\mathrm{u,P}}_{i,k+\kappa}$, the predicted values of $\mathbf{x}^{\mathrm{u}}_{\ell,k+\kappa}$ and $\mathbf{x}^{\mathrm{u}}_{i,k+\kappa}$, for $\kappa = 1,\ldots,h$. Then, using the communication condition (9), the set of UAVs with which UAV i can expect to be able to communicate at time $k+\kappa$, $\kappa = 1,\ldots,h$, is

$$\mathcal{N}^{\mathrm{P}}_{i,k+\kappa} = \left\{\ell \in \mathcal{N}^{\mathrm{C}}_{i,k} \mid c\left(\mathbf{x}^{\mathrm{u,P}}_{i,k+\kappa}, \mathbf{x}^{\mathrm{u,P}}_{\ell,k+\kappa}\right) \geqslant 0\right\}. \tag{48}$$

If $\mathbf{x}^{\mathrm{u}}_{i,k+\kappa} = \mathbf{x}^{\mathrm{u,P}}_{i,k+\kappa}$ and $\mathbf{x}^{\mathrm{u}}_{\ell,k+\kappa} = \mathbf{x}^{\mathrm{u,P}}_{\ell,k+\kappa}$, $\ell \in \mathcal{N}_{i,k}$, $\kappa = 1,\ldots,h$, the set $\mathcal{N}^{\mathrm{P}}_{i,k+\kappa}$ is a subset of $\mathcal{N}_{i,k+\kappa}$, since UAVs that are not in $\mathcal{N}^{\mathrm{C}}_{i,k}$ may also be able to communicate with UAV i at time $k+\kappa$, $\kappa = 1,\ldots,h$.

At time $k+\kappa$, for the correction step from communications, we consider that UAV i is only allowed to account for the FoV $\mathbb{F}_\ell(\mathbf{x}^{\mathrm{u,P}}_{\ell,k+\kappa})$ of UAVs with index $\ell \in \mathcal{N}^{\mathrm{P}}_{i,k+\kappa}$. All information that the neighbors of UAV i may receive from their own neighbors, not belonging to $\mathcal{N}^{\mathrm{P}}_{i,k+\kappa}$ is thus ignored.

At time k, UAV i can compute $\mathbb{X}^{\mathrm{A}}_{i,k}$ using (43). Applying the prediction step (44) and correction step from measurements (46), we get $\mathbb{X}^{\mathrm{A,P}}_{i,k+1|k}$ and $\mathbb{X}^{\mathrm{A,P}}_{i,k+1|k+1}$. UAV i will receive $\mathbf{x}^{\mathrm{u}}_{\ell,k}$ and $\mathbf{u}_{\ell,k}$ from all UAVs with index $\ell \in \mathcal{N}^{\mathrm{P}}_{i,k+1}$, from which the FOV $\mathbb{F}_\ell(\mathbf{x}^{\mathrm{u,P}}_{\ell,k+1})$ is deduced. Ignoring possible detection of new or previously detected targets in $\mathbb{F}_\ell(\mathbf{x}^{\mathrm{u,P}}_{\ell,k+1})$, UAV i simply accounts for the reduction of the size of the search space provided by $\mathbb{F}_\ell(\mathbf{x}^{\mathrm{u,P}}_{\ell,k+1})$, $\ell \in \mathcal{N}^{\mathrm{P}}_{i,k+1}$, to evaluate $\mathbb{X}^{\mathrm{A,P}}_{i,k+1}$ similarly to (46), so as to get

$$\mathbb{X}^{\mathrm{A,P}}_{i,k+1} = \mathbb{X}^{\mathrm{A}}_{i,k+1|k+1} \setminus \bigcup_{\ell\in\mathcal{N}^{\mathrm{P}}_{i,k+1}} \mathbb{F}_\ell\left(\mathbf{x}^{\mathrm{u,P}}_{\ell,k+1}\right). \tag{49}$$

In this SM-MPC approach, UAV i processes the FoVs of its neighbors as its own FoV.

As in 5.1, this process may be iterated from $\mathbb{X}^{\mathrm{A,P}}_{i,k+\kappa-1}$ to further evaluate the impact on $\mathbb{X}^{\mathrm{A,P}}_{i,k+\kappa}$ of $\mathbf{u}_{i,k+\kappa-1}$ as well as $\mathbf{u}_{\ell,k+\kappa-1}$, $\ell \in \mathcal{N}^{\mathrm{C}}_{i,k}$ and $\kappa = 2,\ldots,h$. UAV i then searches the sequence of control inputs $\left(\mathbf{u}_{i,k},\ldots,\mathbf{u}_{i,k+h-1}\right)$ minimizing (47).

5.3. Practical issues

The order in which the UAVs compute their control inputs at each time step k has to be determined. Assume that UAV i has access to $\mathcal{N}_{i,k}$ from previous communication. The considered suboptimal distributed approach for UAV i is to compute its control inputs only once it has received the predicted control inputs from all UAVs in $\mathcal{N}_{i,k}$ with a smaller index, *i.e.*, from all UAVs with index in $\mathcal{N}^{\mathrm{C}}_{i,k} \subset \mathcal{N}_{i,k}$.

In each $\mathcal{N}_{i,k}$, $i = 1,\ldots,N_{\mathrm{u}}$, UAV i is able to determine whether it has the smallest index. If this is the case, UAV i evaluates and communicates its control input

$$\left(\widehat{\mathbf{u}}_{1,k},\ldots,\widehat{\mathbf{u}}_{1,k+h-1}\right) = \arg\min J\left(\mathbb{X}^{\mathrm{A,P}}_{i,k+h}, \mathbf{x}^{\mathrm{u,P}}_{i,k+h}\right),$$

where the minimization is over all $\mathbf{u}_{i,k} \in \mathbb{U}_0,\ldots,\mathbf{u}_{i,k+h-1} \in \mathbb{U}_{h-1}$, without accounting for the presence of its neighbors. In practice, to lighten computations, $\mathbb{U}_0,\ldots,\mathbb{U}_{h-1}$ are chosen as discrete subsets of $\mathbb{U}$, the set of admissible control inputs. Then, one of the UAVs with index $\ell \in \mathcal{N}_{i,k}$, $\ell > i$ can determine $\left(\widehat{\mathbf{u}}_{\ell,k},\ldots,\widehat{\mathbf{u}}_{\ell,k+h-1}\right)$ minimizing $J(\mathbb{X}^{\mathrm{A,P}}_{\ell,k+h}, \mathbf{x}^{\mathrm{u,P}}_{\ell,k+h})$, accounting for $\left(\widehat{\mathbf{u}}_{i,k},\ldots,\widehat{\mathbf{u}}_{i,k+h-1}\right)$ provided by UAV i.

6. Simulations

The performance of the proposed approach is evaluated via simulations.

The targets move on the ground with a speed module V^{t} assumed constant. At time k, $(x^{\mathrm{t}}_{j,k,1}, x^{\mathrm{t}}_{j,k,2})^\intercal$ are the coordinates of target j, $x^{\mathrm{t}}_{j,k,3}$ is its heading angle, $x^{\mathrm{t}}_{j,k,4}$ its yaw rate. The yaw rate derivative $x^{\mathrm{t}}_{j,k,5}$ follows a random walk with input $v_{j,k}$ uniformly distributed in the interval $[-\pi/8, \pi/8]\ \mathrm{s}^{-2}$, *i.e.*, $v_{j,k} \sim \mathcal{U}\left(-\pi/8\ \mathrm{s}^{-2}, \pi/8\ \mathrm{s}^{-2}\right)$. The target state vector $\mathbf{x}^{\mathrm{t}}_{j,k}$ evolves according to

$$\begin{pmatrix} x^{\mathrm{t}}_{j,k+1,1} \\ x^{\mathrm{t}}_{j,k+1,2} \\ x^{\mathrm{t}}_{j,k+1,3} \\ x^{\mathrm{t}}_{j,k+1,4} \\ x^{\mathrm{t}}_{j,k+1,5} \end{pmatrix} = \begin{pmatrix} x^{\mathrm{t}}_{j,k,1} + T^{\mathrm{d}} \cos\left(x^{\mathrm{t}}_{j,k,3}\right) V^{\mathrm{t}} \\ x^{\mathrm{t}}_{j,k,2} + T^{\mathrm{d}} \sin\left(x^{\mathrm{t}}_{j,k,3}\right) V^{\mathrm{t}} \\ x^{\mathrm{t}}_{j,k,3} + T^{\mathrm{d}} x^{\mathrm{t}}_{j,k,4} \\ x^{\mathrm{t}}_{j,k,4} + T^{\mathrm{d}} x^{\mathrm{t}}_{j,k,5} \\ v_{j,k} \end{pmatrix},$$

where $T^{\mathrm{d}} = 0.05\,\mathrm{s}$. The state of UAV i at time k consists of its coordinates $(x^{\mathrm{u}}_{i,k,1}, x^{\mathrm{u}}_{i,k,2}, x^{\mathrm{u}}_{i,k,3})^\intercal$, flight path angle $x^{\mathrm{u}}_{i,k,4}$, heading angle $x^{\mathrm{u}}_{i,k,5}$, yaw rate $x^{\mathrm{u}}_{i,k,6}$, and yaw rate derivative $x^{\mathrm{t}}_{i,k,7}$. The

control input is applied to $x^{\mathrm{u}}_{i,k,7}$. The UAV state vector $\mathbf{x}^{\mathrm{u}}_{i,k}$ evolves according to

$$\begin{pmatrix} x^{\mathrm{u}}_{i,k+1,1} \\ x^{\mathrm{u}}_{i,k+1,2} \\ x^{\mathrm{u}}_{i,k+1,3} \\ x^{\mathrm{u}}_{i,k+1,4} \\ x^{\mathrm{u}}_{i,k+1,5} \\ x^{\mathrm{u}}_{i,k+1,6} \\ x^{\mathrm{u}}_{i,k+1,7} \end{pmatrix} = \begin{pmatrix} x^{\mathrm{u}}_{i,k,1} + T^{\mathrm{d}} \cos\left(x^{\mathrm{u}}_{i,k,4}\right) \cos\left(x^{\mathrm{u}}_{i,k,5}\right) V^{\mathrm{u}} \\ x^{\mathrm{u}}_{i,k,2} + T^{\mathrm{d}} \cos\left(x^{\mathrm{u}}_{i,k,4}\right) \sin\left(x^{\mathrm{u}}_{i,k,5}\right) V^{\mathrm{u}} \\ x^{\mathrm{u}}_{i,k,3} + T^{\mathrm{d}} \sin\left(x^{\mathrm{u}}_{i,k,4}\right) V^{\mathrm{u}} \\ x^{\mathrm{u}}_{i,k,4} \\ x^{\mathrm{u}}_{i,k,5} + T^{\mathrm{d}} x^{\mathrm{t}}_{i,k,6} \\ x^{\mathrm{u}}_{i,k,6} + T^{\mathrm{d}} x^{\mathrm{t}}_{i,k,7} \\ u_{i,k} \end{pmatrix}.$$

The altitude $x^{\mathrm{u}}_{i,k,3} = 100\,\mathrm{m}$, the flight path angle $x^{\mathrm{u}}_{i,k,4} = 0$, and the speed module $V^{\mathrm{u}} = 16.6$ m/s are assumed constant.

The UAVs are equipped with identical optical sensors able to detect targets within their FoV. The sensor opening angles are equal to $\pi/4$ in both azimuth and elevation. A noisy measurement $\mathbf{y}_{i,j,k}$ of $(x^{\mathrm{t}}_{j,k,1}, x^{\mathrm{t}}_{j,k,2})^{\intercal}$ is obtained with a noise $\mathbf{w}_{i,j,k} \sim \mathcal{U}(-5\,\mathrm{m}, 5\,\mathrm{m})$ when a target is detected, as described by (5) and (6). A target is detected and identified at time k when (3) is satisfied, where

$$g^{\mathrm{t}}_j\left(\mathbf{x}^{\mathrm{u}}_{i,k}, \mathbf{x}^{\mathrm{t}}_{j,k}\right) = \left(\mathbf{x}^{\mathrm{u}}_{i,k} - \mathbf{x}^{\mathrm{t}}_{j,k}\right)^{\intercal} \mathbf{a}^{\mathrm{t}}_{j,k} - \left\|\mathbf{x}^{\mathrm{u}}_{i,k} - \mathbf{x}^{\mathrm{t}}_{j,k}\right\| \left\|\mathbf{a}^{\mathrm{t}}_{j,k}\right\| \left(\cos\lambda^{\mathrm{t}}_j\right) \tag{50}$$

represents a half circular cone of $\mathbb{R}^3$ with a small aperture $2\lambda^{\mathrm{t}}_j = \pi/60$, to make identification of targets more difficult. The cone vertex is $\mathbf{x}^{\mathrm{t}}_{j,k}$ and its axis is

$$\mathbf{a}^{\mathrm{t}}_{j,k} = \left(\sin\gamma_j \cos\left(x^{\mathrm{t}}_{j,k,3} + \beta_j\right), \sin\gamma_j \sin\left(x^{\mathrm{t}}_{j,k,3} + \beta_j\right), \cos\gamma_j, 0, 0, 0\right)^{\intercal}, \tag{51}$$

with azimuth $\beta_j \sim \mathcal{U}(-\pi/4, \pi/4)$ and elevation angle $\gamma_j \sim \mathcal{U}(2\pi/60, 3\pi/60)$.

The false targets evolve according to the same dynamics as the true targets. False targets are detected and misidentified when (4) is satisfied, where

$$g^{\mathrm{f}}_\ell\left(\mathbf{x}^{\mathrm{u}}_{i,k}, \mathbf{x}^{\mathrm{f}}_{\ell,k}\right) = \left(\mathbf{x}^{\mathrm{u}}_{i,k} - \mathbf{x}^{\mathrm{f}}_{\ell,k}\right)^{\intercal} \mathbf{a}^{\mathrm{f}}_{\ell,k} - \left\|\mathbf{x}^{\mathrm{u}}_{i,k} - \mathbf{x}^{\mathrm{f}}_{\ell,k}\right\| \left\|\mathbf{a}^{\mathrm{f}}_{\ell,k}\right\| \left(\cos\lambda^{\mathrm{f,g}}_\ell\right) \tag{52}$$

and

$$q^{\mathrm{f}}_\ell\left(\mathbf{x}^{\mathrm{u}}_{i,k}, \mathbf{x}^{\mathrm{f}}_{\ell,k}\right) = \left(\mathbf{x}^{\mathrm{u}}_{i,k} - \mathbf{x}^{\mathrm{f}}_{\ell,k}\right)^{\intercal} \mathbf{a}^{\mathrm{f}}_{\ell,k} - \left\|\mathbf{x}^{\mathrm{u}}_{i,k} - \mathbf{x}^{\mathrm{f}}_{\ell,k}\right\| \left\|\mathbf{a}^{\mathrm{f}}_{\ell,k}\right\| \left(\cos\lambda^{\mathrm{f,q}}_\ell\right), \tag{53}$$

where $2\lambda^{\mathrm{f,g}}_\ell = \pi/30$ and $2\lambda^{\mathrm{f,q}}_\ell = \pi/60$. In both cases,

$$\mathbf{a}^{\mathrm{f}}_{\ell,k} = \left(\sin\gamma_\ell \cos\left(x^{\mathrm{f}}_{\ell,k,3} + \beta_\ell\right), \sin\gamma_\ell \cdot \sin\left(x^{\mathrm{f}}_{\ell,k,3} + \beta_\ell\right), \cos\gamma_\ell, 0, 0, 0\right)^{\intercal}, \tag{54}$$

with $\beta_\ell \sim \mathcal{U}(-\pi/4, \pi/4)$ and $\gamma_\ell \sim \mathcal{U}(2\pi/60, 3\pi/60)$.

In the communication condition (9),

$$c\left(\mathbf{x}^{\mathrm{u}}_{i,k}, \mathbf{x}^{\mathrm{u}}_{\ell,k}\right) = d^{\mathrm{c}} - d\left(\mathbf{x}^{\mathrm{u}}_{i,k}, \mathbf{x}^{\mathrm{u}}_{\ell,k}\right),$$

where $d^{\mathrm{c}} = 200\,\mathrm{m}$ is the maximum communication range and $d\left(\mathbf{x}^{\mathrm{u}}_{i,k}, \mathbf{x}^{\mathrm{u}}_{\ell,k}\right)$ is the distance between UAV i and ℓ. The communication delays are neglected. The prediction horizon for the SM-MPC is $h = 2$. The control input is computed with a period $T^{\mathrm{c}} = 0.5\,\mathrm{s}$ equal to the communication period.

The search area is a square of $400 \times 400\ \mathrm{m}^2$. The simulations have been carried out in Matlab. Matlab's *polyshapes* are used to represent sets. Polyshapes simplify the handling of sets in $\mathbb{R}^2$ regarding Boolean and geometrical operations. In higher-dimensions subpavings, *i.e.*, unions of non-overlapping interval vectors (Kieffer et al., 2002) can be used.

The parameter of the cost function (47) is $\alpha = 0.0001$, to give more importance to the reduction of the set estimates.

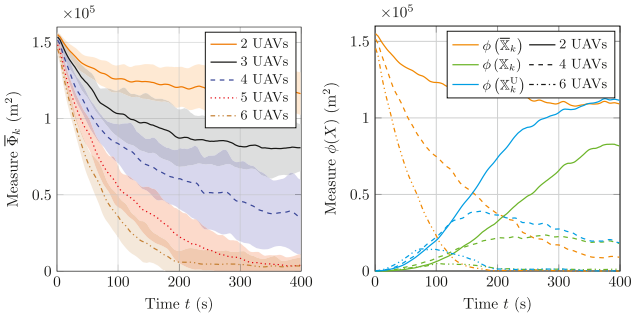

Fig. 8. Left: Mean values (line) and standard deviation (shaded area) of $\overline{\Phi}_k$ evaluated for 30 simulations with 3 true targets, 3 false targets, and 2 to 6 UAVs. Right: Mean values of $\phi\left(\overline{\mathbb{X}}_k\right)$, $\phi\left(\mathbb{X}^{\mathrm{U}}_k\right)$, and $\phi\left(\mathbb{X}_k\right)$ evaluated with 3 true and 3 false targets, considering 2, 4 and 6 UAVs.

Video sequences associated to the simulations are at https://drive.google.com/drive/folders/1lFtrPrR0J2uXHquSRiZU2FSydXFXIPcB?usp=sharing

The results for each setup of the following simulations were obtained for 30 independent simulations with uniformly distributed initial locations of the targets and UAVs.

Impact of the fleet size

Fig. 8 (left) shows, for different numbers N_{u} of UAVs, the average value and standard deviation of $\overline{\Phi}_k$ as defined in (11), considering 3 true and 3 false targets with $V^{\mathrm{t}} = 1\,\mathrm{m\,s^{-1}}$.

Fig. 8 (right) details the contribution of $\phi\left(\overline{\mathbb{X}}_k\right) = \sum_{i=1}^{N_{\mathrm{u}}} \phi\left(\overline{\mathbb{X}}_{i,k}\right)/N_{\mathrm{u}}$, $\phi\left(\mathbb{X}^{\mathrm{U}}_k\right) = \sum_{i=1}^{N_{\mathrm{u}}} \phi\left(\mathbb{X}^{\mathrm{U}}_{i,k}\right)/N_{\mathrm{u}}$, and $\phi\left(\mathbb{X}_k\right) = \sum_{i=1}^{N_{\mathrm{u}}} \phi\left(\bigcup_{\mathbb{X}_{i,j,k} \in \mathcal{X}_{i,k}} \mathbb{X}_{i,j,k}\right)/N_{\mathrm{u}}$ to $\overline{\Phi}_k$.

Considering the size of the search area and the relative speed of UAVs and of targets, within 400 s, from Fig. 8, at least 5 UAVs are necessary to eliminate $\overline{\mathbb{X}}_{i,k}$. Fig. 8 (right) shows that the growth of $\overline{\mathbb{X}}_{i,k}$ between consecutive observations is too fast to allow 3 UAVs or less to fully eliminate it. The variance of the estimation uncertainty $\overline{\Phi}_k$ is the largest for 4 UAVs: $\phi\left(\overline{\mathbb{X}}_{i,k}\right)$ may or may not converge to 0 depending on the simulations. Videos illustrate both cases (see video FleetSize_4_1 and FleetSize_4_2).

The initial growth of $\phi\left(\mathbb{X}^{\mathrm{U}}_k\right)$ in Fig. 8 (right) is always faster then the initial growth of $\phi\left(\mathbb{X}_k\right)$ since initially, targets are more likely to be unidentified: target identification requires additional measurements. When $\overline{\Phi}_k$ converges to 0, the size of $\mathbb{X}^{\mathrm{U}}_k$ also converges to 0 at some time instant when all false targets are identified and removed from $\mathbb{X}^{\mathrm{U}}_k$, and all true targets are identified and belong to $\mathbb{X}_k$.

Additionally, the video FleetSize_10_1 shows the performance of 10 UAVs tracking 10 true and 10 false targets.

Impact of the target speed

Fig. 9 (left) shows the evolution of $\overline{\Phi}_k$ for different values of V^{t}. The simulations are carried out with 3 true targets, 3 false targets, and 6 UAVs.

The relative speed of targets and UAVs significantly impacts the value to which $\overline{\Phi}_k$ converges. When $V^{\mathrm{t}} = 1.8\,\mathrm{m\,s^{-1}}$, in all simulations, $\phi\left(\overline{\mathbb{X}}_k\right)$ does not converge to 0. When $V^{\mathrm{t}} = 1.6\,\mathrm{m\,s^{-1}}$, $\phi\left(\overline{\mathbb{X}}_k\right)$ converges to 0 only in some simulations (see video TargetSpeed_1).

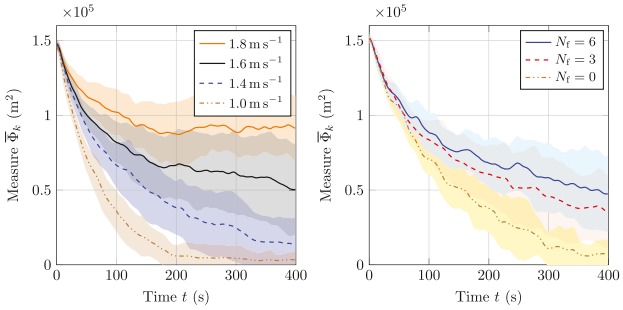

Fig. 9. Mean values (line) and standard deviation (shaded area) of $\overline{\Phi}_k$ evaluated with 3 true targets as well as (left) 6 UAVs, 3 false targets, and different values of the target speed module V^{t}, (right) 4 UAVs, from 0 to 6 false targets, and $V^{\mathrm{t}} = 1\,\mathrm{m\,s^{-1}}$.

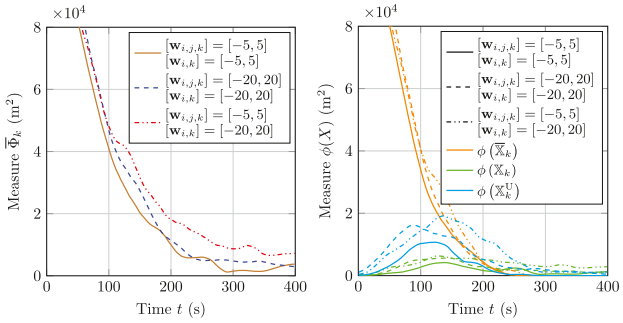

Fig. 10. Mean value of $\overline{\Phi}_k$ (left) and of $\phi\left(\overline{\mathbb{X}}_k\right)$, $\phi\left(\mathbb{X}_k^{\mathrm{U}}\right)$, and $\phi\left(\mathbb{X}_k\right)$ (right) evaluated for 30 simulations with 3 true targets, 0 false targets, and 5 UAVs for different measurement noise bounds $[\mathbf{w}_{i,j,k}]$ and different assumptions $[\mathbf{w}_{i,k}]$ on $[\mathbf{w}_{i,j,k}]$.

Impact of the number of false targets

Fig. 9 (right) shows the evolution of $\overline{\Phi}_k$ for 0, 3, and 6 of false targets. The simulations are carried out with 3 true targets, 4 UAVs, and $V^{\mathrm{t}} = 1\,\mathrm{m\,s^{-1}}$. The convergence speed of $\overline{\Phi}_k$ is affected by an increased N_{f}. This phenomenon is mainly due to an increase of $\phi\left(\mathbb{X}_k^{\mathrm{U}}\right)$ with N_{f}.

Mismatch of the measurement noise bounds

Fig. 10 shows the mean of $\overline{\Phi}_k$ for different values for the measurement noise bounds $[\mathbf{w}_{i,j,k}]$ and different assumptions on the box $[\mathbf{w}_{i,k}]$, known to the UAVs, such that $[\mathbf{w}_{i,j,k}] \subset [\mathbf{w}_{i,k}]$. One considers 3 true targets, 0 false targets, 5 UAVs, and $V^{\mathrm{t}} = 1\,\mathrm{m\,s^{-1}}$.

For small values of t, the decreases of $\overline{\Phi}_k$ are similar, since initially they are mainly due to the decreases of $\phi\left(\overline{\mathbb{X}}_k\right)$. When $t \geqslant 100$ s, the curve of $\overline{\Phi}_k$ obtained for $[\mathbf{w}_{i,j,k}] = [\mathbf{w}_{i,k}] = [-20\,\mathrm{m}, 20\,\mathrm{m}]$ is above that for $[\mathbf{w}_{i,j,k}] = [\mathbf{w}_{i,k}] = [-5\,\mathrm{m}, 5\,\mathrm{m}]$ since large noise bounds lead to larger values of $\phi\left(\mathbb{X}_k^{\mathrm{U}}\right)$ and $\phi\left(\mathbb{X}_k\right)$, as observed in Fig. 10 (right). A mismatch of $[\mathbf{w}_{i,j,k}]$ and $[\mathbf{w}_{i,k}]$ leads to the slowest decrease of $\overline{\Phi}_k$, due to the overestimation of $[\mathbf{w}_{i,j,k}]$ which does not allow an efficient reduction of $\phi\left(\mathbb{X}_k^{\mathrm{U}}\right)$ and $\phi\left(\mathbb{X}_k\right)$ when measurements are exploited.

The simulations show that the state of a true target was never outside the set estimates in any simulation as long as $[\mathbf{w}_{i,j,k}] \subset [\mathbf{w}_{i,k}]$. If $[\mathbf{w}_{i,j,k}] \not\subseteq [\mathbf{w}_{i,k}]$ then all targets are lost at some time instant, which provides a mean to detect erroneous estimates of the noise bounds.

The video NoiseBoundMismatch_1 shows the performance of the state estimator for a large mismatch of $[\mathbf{w}_{i,j,k}]$ and $[\mathbf{w}_{i,k}]$.

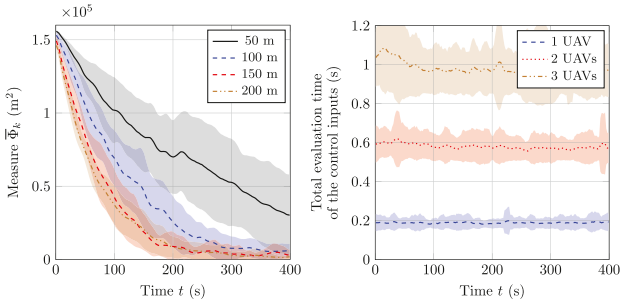

Fig. 11. Mean values (line) and standard deviation (shaded area) of $\overline{\Phi}_k$ evaluated for different values of the communication distances d^{c} when 6 UAVs are exploring an area with 3 true targets and 3 false targets (left), and of the computation time of the control inputs for 1 to 3 UAVs with 3 true targets and no false targets (right), average over 30 simulations.

Impact of the communication distance

Fig. 11 (left) illustrates the detrimental impact of a reduced communication range between UAVs on the decrease speed of $\overline{\Phi}_k$ when 6 UAVs are exploring an area with 3 true targets and 3 false targets. The reduction of d^{c} leads to a less efficient information sharing and thus to a redundant exploration of some areas by several UAVs unaware that these areas were already explored. A video illustrates the performance of the fleet when $d^{\mathrm{c}} = 50$ m (see video ComDist_50).

Processing time of the control input

Fig. 11 (right) shows the mean and standard deviation of the evaluation time of the control input with 3 true targets, no false target and from 1 to 3 UAVs with $V^{\mathrm{t}} = 1\,\mathrm{m\,s^{-1}}$.

One observes that the average total computing time is almost constant with time. The computing times for 2 and 3 UAVs is about three and five times that with a single UAV. This is due to the fact that in the predictive control scheme, once UAV 1 has computed its control input, UAV 2 will have to evaluate the impact of this control input when evaluating its own control input, while UAV 3 will have to evaluate the impact of the control inputs of UAVs 1 and 2.

The video SimpleBaselineMPC_1 shows the performance of the search and track task when the evolution of the set estimates and the control input from the neighbors are not taken into account in the control design.

7. Conclusions and perspectives

This paper presents a distributed set-membership approach to search and track targets using a cooperative fleet of UAVs. The presence of false targets, which may be confused with true targets, is taken into account. When a target is detected in the field of view of a UAV, it is identified as a true or false target only when observed under specific conditions. In the proposed set-membership approach, each UAV maintains several set estimates: one for each detected and identified true target, one for detected but not yet identified targets, and one for not yet detected target.

This last set estimate corresponds to the subset of the state space still to be explored. Using the information available to each UAV (coming from its sensors and information shared by its neighbors), these set estimates are updated so that, at each time step, UAVs can have estimates as precise as possible of the states of tracked targets.

A distributed set-membership model predictive control approach is considered to compute the trajectories of UAVs. The evolution of the set estimates for each UAV is evaluated accounting for the impact of its own future measurements and of future measurements shared by its neighbors. The control inputs minimize a measure of the volume of the set-membership estimates predicted h-step ahead.

Simulation results show the efficiency of the proposed approach. The impact on its convergence of the relative speed of targets and UAVs, of the number of UAVs and of false targets, of the communication range, as well as of the considered measurement noise bounds is evaluated.

In the experimental part, the UAVs were evolving at a constant altitude. Allowing UAVs to adjust their altitude is possible in the proposed framework but requires a refined model of the dependency with altitude of the detection and identification conditions and the measurement noise bounds.

Further extensions of this paper include developing displacement strategies for UAVs to see the potential targets under different points of view to determine whether it is a true or a false target. Other extensions would be to deal with a probability of non-detection within the field of view.

References

Baek, S., & York, G. (2020). Optimal sensor management for multiple target tracking using cooperative unmanned aerial vehicles. In *Proc. IEEE ICUAS* (pp. 1294–1300). IEEE.

Bar-Shalom, Y., Willett, P., & Tian, X. (2011). *Tracking and data fusion*. YBS publishing Storrs, USA.

Bemporad, A., & Garulli, A. (2000). Output-feedback predictive control of constrained linear systems via set-membership state estimation. *International Journal of Control*, *73*(8), 655–665.

Bertuccelli, L. F., & How, J. (2005). Robust UAV search for environments with imprecise probability maps. In *Proc. 44th IEEE CDC* (pp. 5680–5685). IEEE.

Blasch, E., & Kahler, B. (2005). Multiresolution EO/IR target tracking and identification. In *Proc. 7th international conference on information fusion, Vol. 1* (pp. 8–pp). IEEE.

Camacho, E., & Alba, C. (2013). *Model predictive control*. Springer Science & Business Media.

Canale, M., Fagiano, L., & Signorile, M. C. (2014). Nonlinear model predictive control from data: a set membership approach. *International Journal of Robust and Nonlinear Control*, *24*(1), 123–139.

Cortes, J., Martinez, S., Karatas, T., & Bullo, F. (2004). Coverage control for mobile sensing networks. *Transactions on Robotics and Automation*, *20*(2), 243–255.

Dames, P. (2017). Distributed multi-target search and tracking using the PHD filter. In *Proc. int. symp. on multi-robot and multi-agent systems* (pp. 1–8). IEEE.

Drevelle, V., Jaulin, L., & Zerr, B. (2013). Guaranteed characterization of the explored space of a mobile robot by using subpavings. In *Proc. IFAC NOLCOS* (pp. 44–49).

Farmani, N., Sun, L., & Pack, D. (2015). Tracking multiple mobile targets using cooperative unmanned aerial vehicles. In *Proc. IEEE ICUAS* (pp. 395–400). IEEE.

Flint, M., Fernández, E., & Polycarpou, M. (2004). Efficient bayesian methods for updating and storing uncertain search information for UAVs. In *Proc. IEEE CDC* (pp. 1093–1098).

Foraker, J., Royset, J. O., & Kaminer, I. (2016a). Search-trajectory optimization: Part I, formulation and theory. *Journal of Optimization Theory and Applications*, *169*(2), 530–549.

Foraker, J., Royset, J. O., & Kaminer, I. (2016b). Search-trajectory optimization: Part II, algorithms and computations. *Journal of Optimization Theory and Applications*, *169*(2), 550–567.

Gu, F., He, Y., & Han, J. (2015). Active persistent localization of a three-dimensional moving target under set-membership uncertainty description through cooperation of multiple mobile robots. *IEEE Transactions on Industrial Electronics*, *62*(8), 4958–4971.

He, S., Shin, H.-S., & Tsourdos, A. (2017). Constrained multiple model Bayesian filtering for target tracking in cluttered environment. *IFAC-PapersOnLine*, *50*(1), 425–430.

Ibenthal, J., Meyer, L., Kieffer, M., & Piet-Lahanier, H. (2020). Bounded-error target localization and tracking in presence of decoys using a fleet of UAVs. In *Proc. 21th IFAC world congress* (pp. 9521–9528). IFAC-PapersOnLine.

Ibenthal, J., Meyer, L., Piet-Lahanier, H., & Kieffer, M. (2020). Target search and tracking using a fleet of UAVs in presence of decoys and obstacles. In *Proc. 59th IEEE CDC* (pp. 188–194).

Ji, T., & Driggs-Campbell, K. (2020). Robust model predictive control with recursive state estimation under set-membership uncertainty. arxiv preprint arXiv:2008.04980.

Khan, A., Rinner, B., & Cavallaro, A. (2018). Cooperative robots to observe moving targets. *IEEE Transactions on Cybernetics*, *48*(1), 187–198.

Khodayi-mehr, R., Kantaros, Y., & Zavlanos, M. M. (2019). Distributed state estimation using intermittently connected robot networks. *IEEE Transactions on Robotics*, *35*(3), 709–724.

Kieffer, M., Jaulin, L., & Walter, E. (2002). Guaranteed recursive non-linear state bounding using interval analysis. *International Journal of Adaptive Control and Signal Processing*, *16*(3), 193–218.

Kouvaritakis, B., & Cannon, M. (2015). Developments in robust and stochastic predictive control in the presence of uncertainty. *ASCE-ASME Journal of Risk and Uncertainty in Engineering Systems B*, *1*(2).

Li, P., & Duan, H. (2017). A potential game approach to multiple UAV cooperative search and surveillance. *Aerospace Science and Technology*, *68*, 403–415.

Lu, X., Zhang, H., Wang, W., & Teo, K.-L. (2005). Kalman filtering for multiple time-delay systems. *Automatica*, *41*(8), 1455–1461.

Morari, M., & Lee, J. H. (1999). Model predictive control: past, present and future. *Computers & Chemical Engineering*, *23*, 667–682.

Pan, Y., Li, S., Zhang, X., Liu, J., Huang, Z., & Zhu, T. (2017). Directional monitoring of multiple moving targets by multiple unmanned aerial vehicles. In *Proc. IEEE GLOBECOM* (pp. 1–6). IEEE.

Raap, M., Preuß, M., & Meyer-Nieberg, S. (2019). Moving target search optimization–A literature review. *Computers & Operations Research*, *105*, 132–140.

Reboul, L., Kieffer, M., Piet-Lahanier, H., & Reynaud, S. (2019). Cooperative guidance of a fleet of UAVs for multi-target discovery and tracking in presence of obstacles using a set membership approach. In *Proc. IFAC ACA* (pp. 340–345).

Reynaud, S., Kieffer, M., Piet-Lahanier, H., & Reboul, L. (2018). A set-membership approach to find and track multiple targets using a fleet of UAVs. In *Proc. IEEE CDC* (pp. 484–489).

Robin, C., & Lacroix, S. (2016). Multi-robot target detection and tracking: taxonomy and survey. *Autonomous Robots*, *40*(4), 729–760.

Sun, L., Baek, S., & Pack, D. (2014). Distributed probabilistic search and tracking of agile mobile ground targets using a network of unmanned aerial vehicles. In *Human behavior understanding in networked sensing* (pp. 301–319). Springer.

Tokekar, P., Isler, V., & Franchi, A. (2014). Multi-target visual tracking with aerial robots. In *Proc. IROS* (pp. 3067–3072). IEEE.

Yang, Y., Polycarpou, M. M., & Minai, A. A. (2007). Multi-UAV cooperative search using an opportunistic learning method. *Journal of Dynamic Systems, Measurement, and Control*, 716–728.

Zhang, M., Song, J., Huang, L., & Zhang, C. (2017). Distributed cooperative search with collision avoidance for a team of unmanned aerial vehicles using gradient optimization. *Journal of Aerospace Engineering*, *30*(1), Article 04016064.

Julius Ibenthal graduated from Leibniz University Hannover in 2019. He is presently doing his doctorate at the ONERA and University Paris-Saclay. His research interests are set-membership state estimation and cooperative guidance.

Michel Kieffer is a full professor in signal processing for communications at the University Paris-Saclay and a researcher at the Laboratoire des Signaux et Systèmes, Gif-sur-Yvette. From 2009 to 2016, he was part-time invited professor at the Laboratoire Traitement et Communication de l'Information, Telecom Paris, Paris.

His research interests are in signal processing and control techniques for multimedia, communications, and networking, distributed source coding, network coding, joint source-channel coding and decoding, joint source-network coding. Applications are mainly in the reliable delivery of multimedia contents over wireless channels. He is also interested in guaranteed and robust state bounding and distributed control for systems described by non-linear models in a bounded-error context.

Luc Meyer received the Ph.D. degree in automatic control from Paris Saclay University in 2017. He is presently a research engineer at Onera, the French Aerospace Lab. His research interests include set-membership state estimation and observer design.

Hélène Piet-Lahanier is Directeur de Recherche in ONERA department of Information Processing and System where she is Scientific Deputy. She graduated from SupAero (Toulouse) and obtained her Ph.D. in Physics and her Habilitation à Diriger les Recherches (HDR), both from the University Paris Saclay. Her research interests include modeling under uncertainty, bounded error estimation, cooperative guidance and event-triggered estimation. She is a member of the IFAC technical committee on Aerospace.

Sébastien Reynaud graduated from the Paris Sud University, Paris XI in Pure Mathematics. He joined ONERA in 2012 and is currently Head of ONERA's Aerospace Surveillance and Defence Systems Unit. His main research interests are in the field of estimation and tracking with applications to fleet management and space domain awareness. He is in charge of several studies in the field of space situational awareness.